Supporting Information

First-in-class star-shaped triazine dendrimers endowed with MMP-9 inhibition and VEGF suppression capacity; design, synthesis and anticancer evaluation

Nesreen S. Haiba,[a] Hosam H. Khalil,[b] Ahmed Bergas,[b] Marwa M. Abu-Serie,[c]
Sherine N. Khattab,*[b,e] Mohamed Teleb,[d,e]

[a] Department of Physics and Chemistry, Faculty of Education, Alexandria University, Egypt

[b] Chemistry Department, Faculty of Science, Alexandria University, Alexandria 21321, Egypt

[c] Medical Biotechnology Department, Genetic Engineering and Biotechnology Research Institute, City of Scientific Research and Technological Applications (SRTA-City), Egypt

[d] Department of Pharmaceutical Chemistry, Faculty of Pharmacy, Alexandria University, Alexandria, Egypt

[e] Cancer Nanotechnology Research Laboratory (CNRL), Faculty of Pharmacy, Alexandria University, Alexandria, Egypt

Table of Content

1. IR and NMR (^{1}H and ^{13}C) Spectra of the synthesized dendrimers and their precursors.

2. Biological evaluation

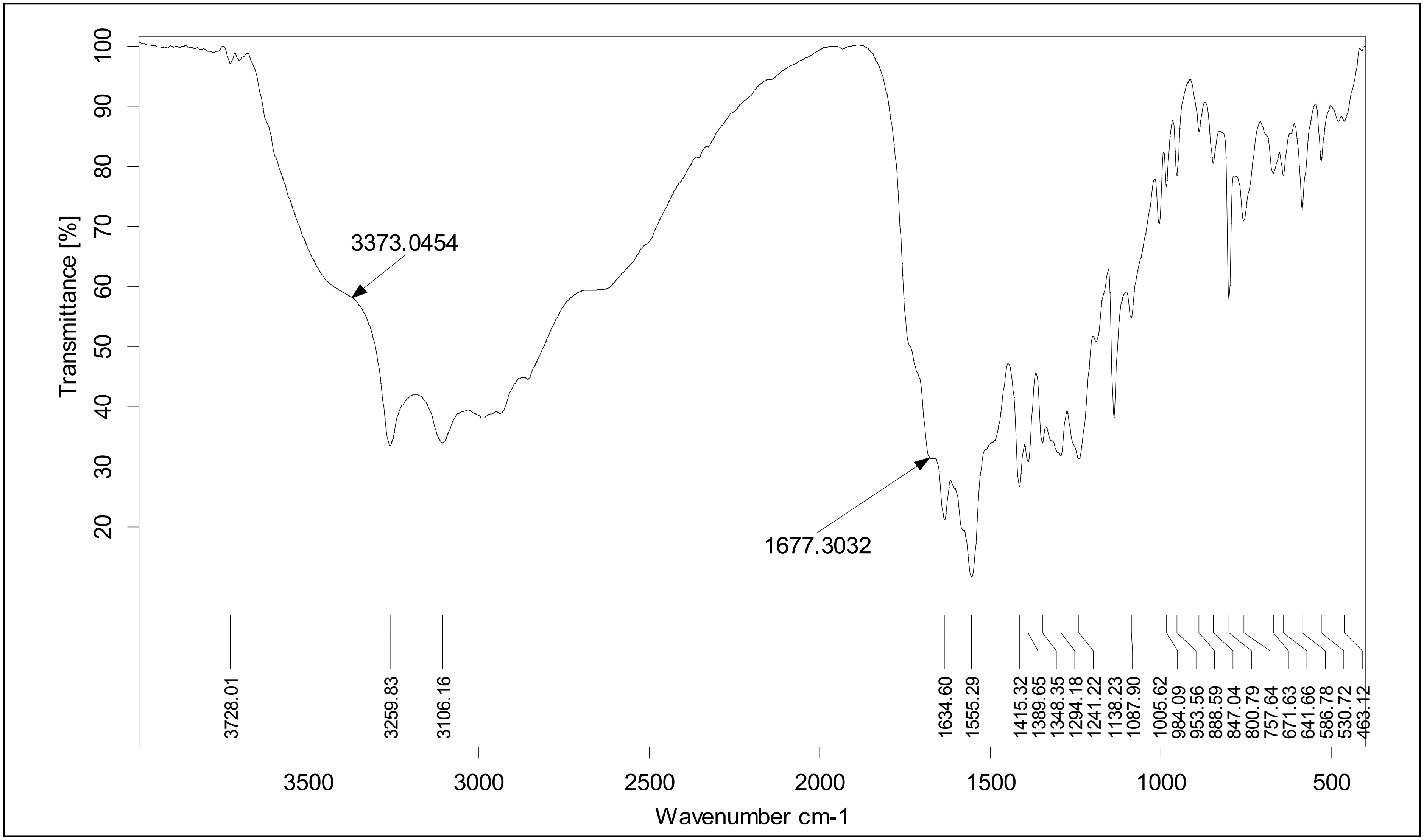

Figure S1: IR (KBr) spectrum of 2,2',2'',2''',2'''',2'''''-((6,6',6''-(2,2',2''-(4,4',4''-((1,3,5-triazine-2,4,6-triyl)tris(azanediyl))tris(benzoyl))tris(hydrazine-2,1-diyl))tris(1,3,5-triazine-6,4,2-triyl))hexakis(azanediyl))hexaacetic acid **8a.**

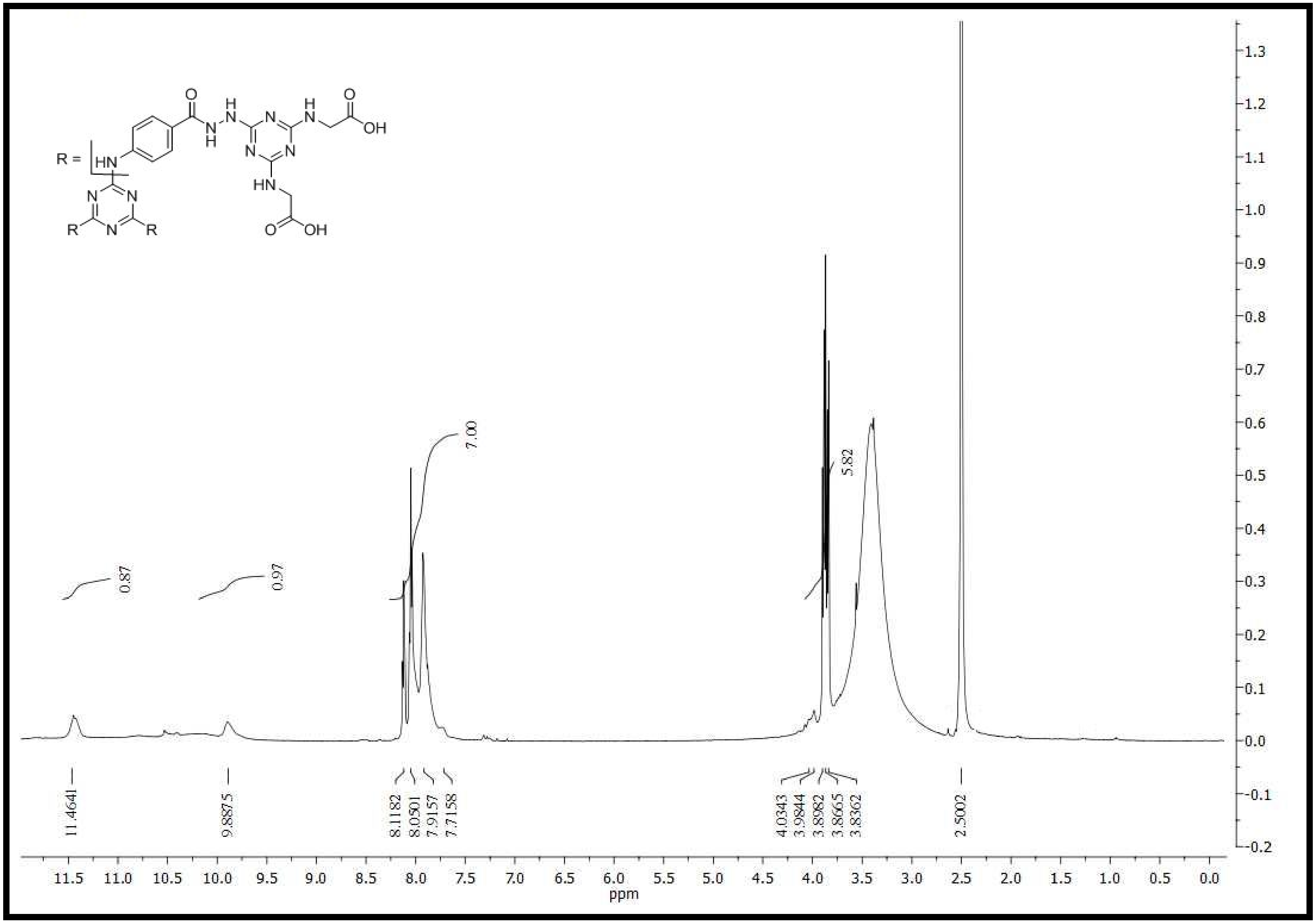

Figure S2: [1]H-NMR (DMSO-d_6) spectrum of 2,2',2'',2''',2'''',2'''''-((6,6',6''-(2,2',2''-(4,4',4''-((1,3,5-triazine-2,4,6-triyl)tris(azanediyl))tris(benzoyl))tris(hydrazine-2,1-diyl))tris(1,3,5-triazine-6,4,2-triyl))hexakis(azanediyl))hexaacetic acid **8a.**

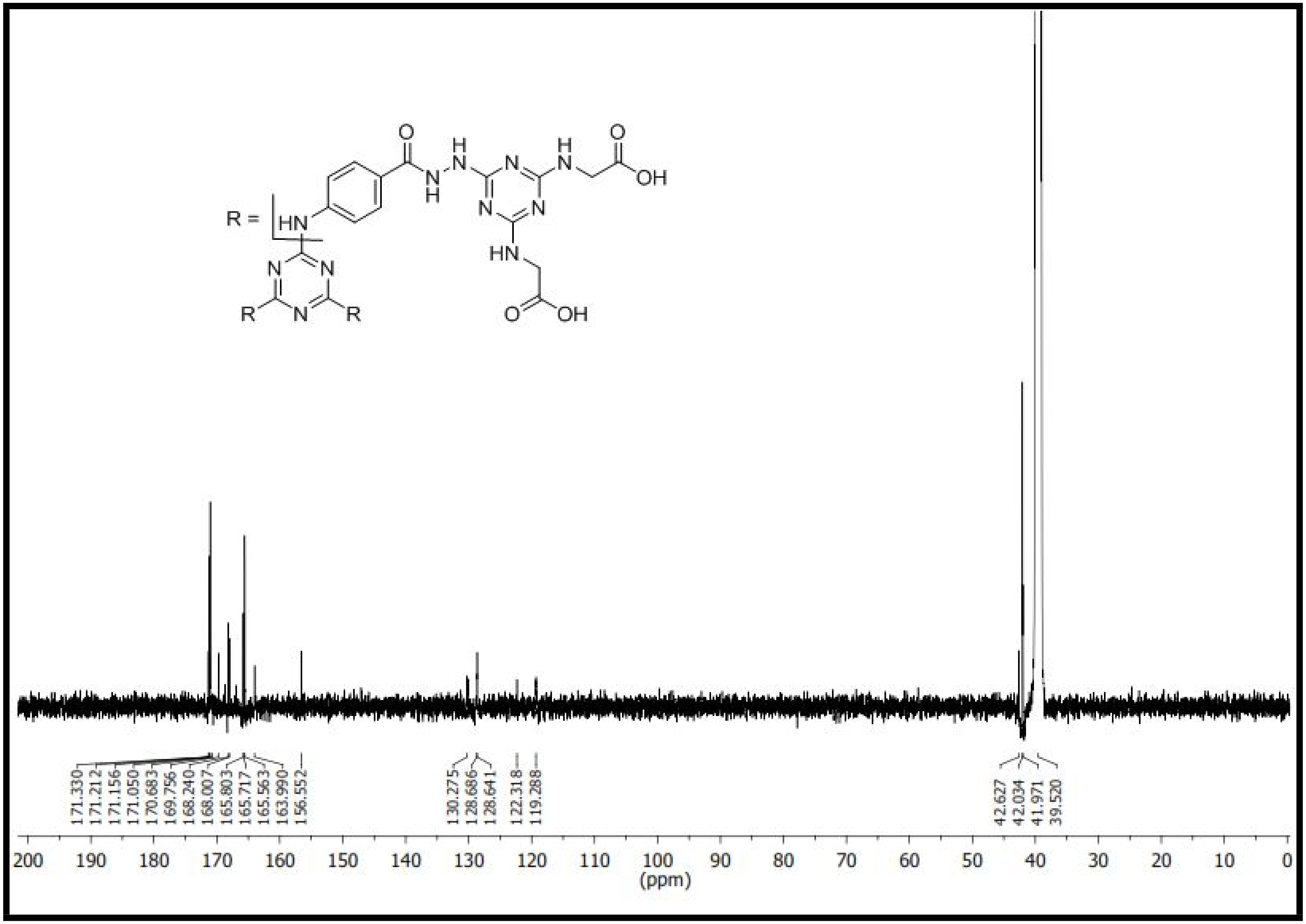

Figure S3: ^{13}C-NMR (DMSO-d_6) spectrum of 2,2',2'',2''',2'''',2'''''-((6,6',6''-(2,2',2''-(4,4',4''-((1,3,5-triazine-2,4,6-triyl)tris(azanediyl))tris(benzoyl)) tris(hydrazine-2,1-diyl))tris(1,3,5-triazine-6,4,2-triyl))hexakis(azanediyl))hexaacetic acid **8a.**

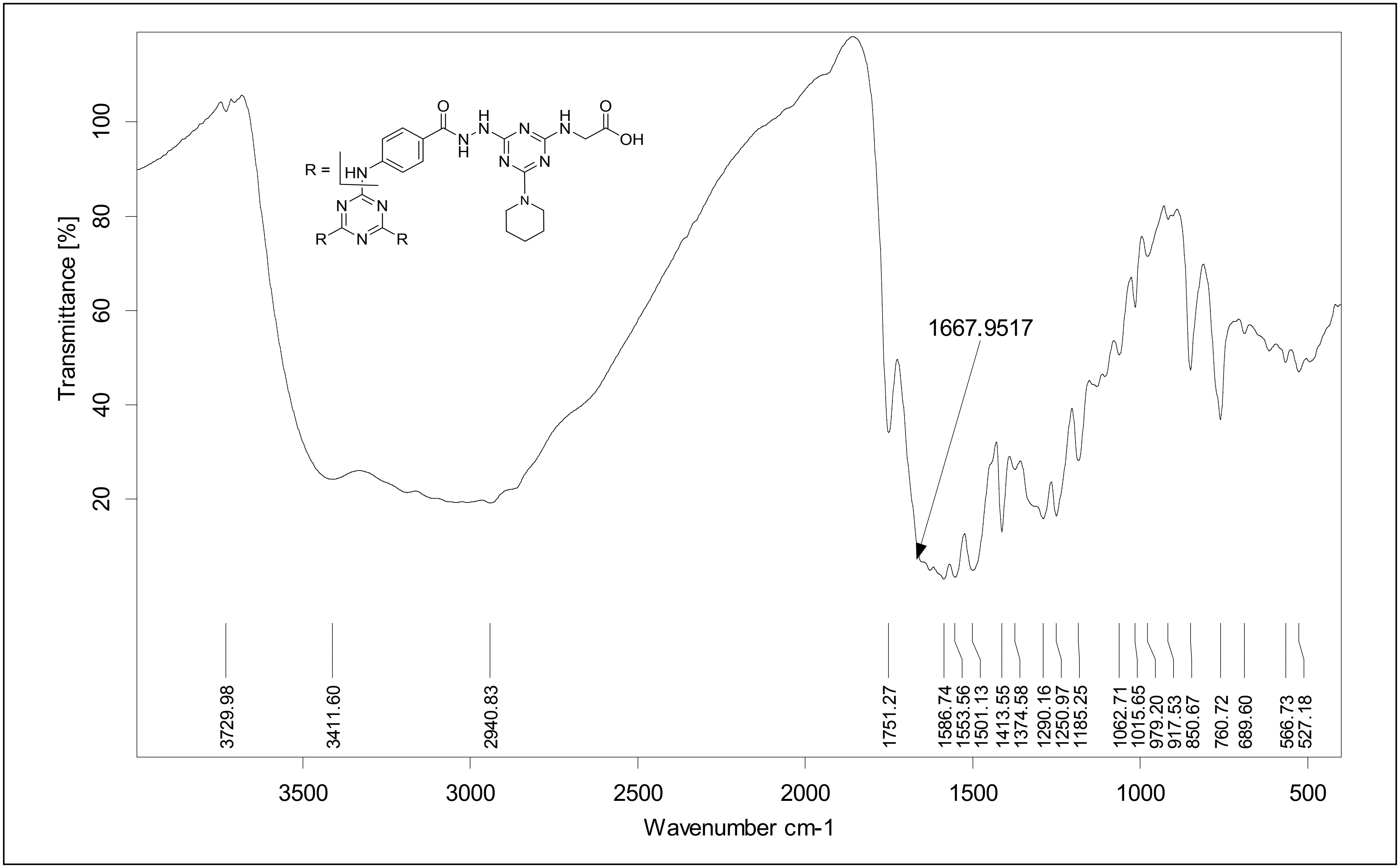

Figure S4: IR (KBr) spectrum of 2,2',2''-((6,6',6''-(2,2',2''-(4,4',4''-((1,3,5-triazine-2,4,6-triyl)tris(azanediyl))tris(benzoyl))tris(hydrazine-2,1-diyl))tris(4-(piperidin-1-yl)-1,3,5-triazine-6,2-diyl))tris(azanediyl))triacetic acid **8b.**

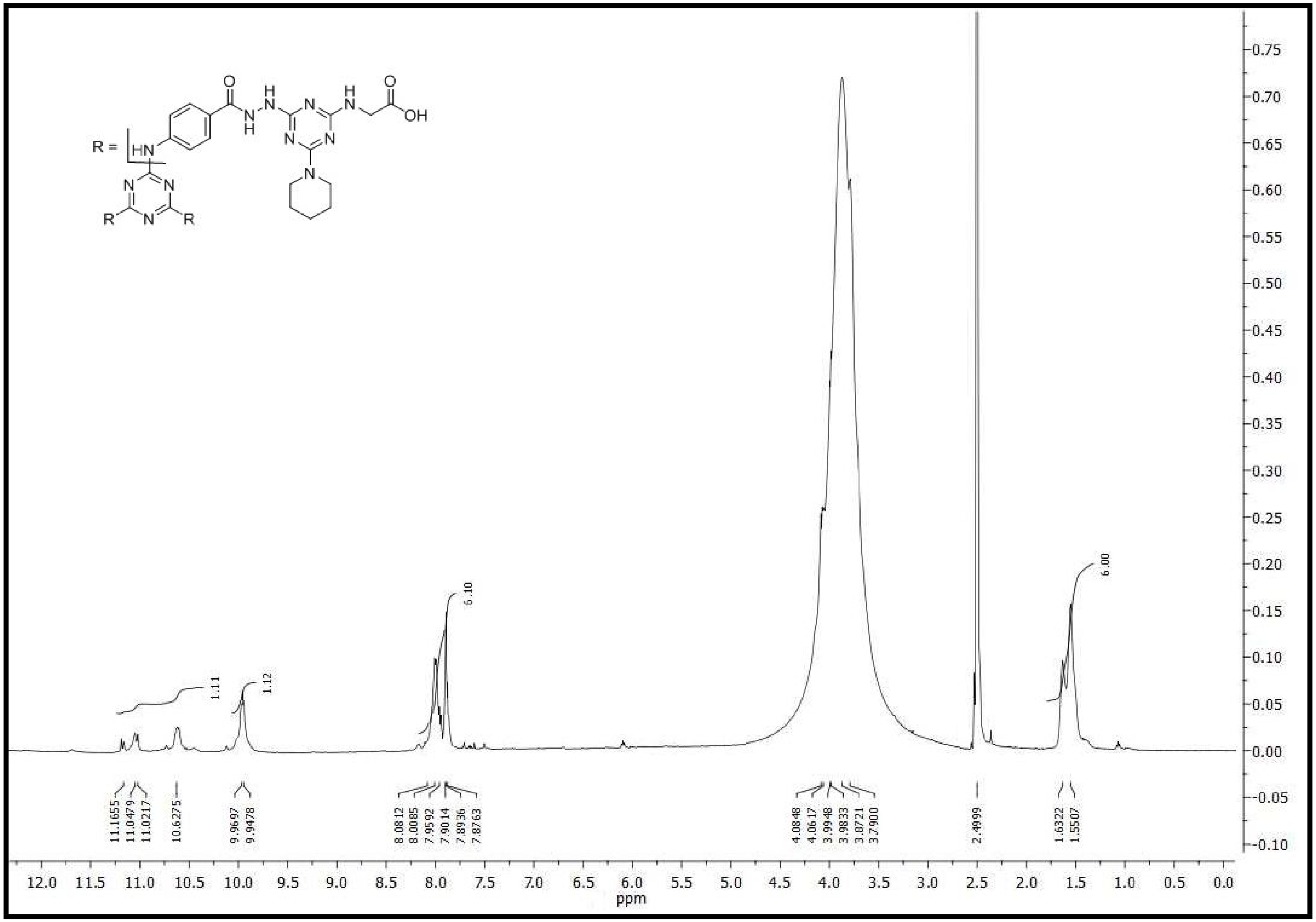

Figure S5: [1]H-NMR (DMSO-d_6) spectrum of 2,2',2''-((6,6',6''-(2,2',2''-(4,4',4''-((1,3,5-triazine-2,4,6-triyl)tris(azanediyl))tris(benzoyl))tris(hydrazine-2,1-diyl))tris(4-(piperidin-1-yl)-1,3,5-triazine-6,2-diyl))tris(azanediyl))triacetic acid **8b.**

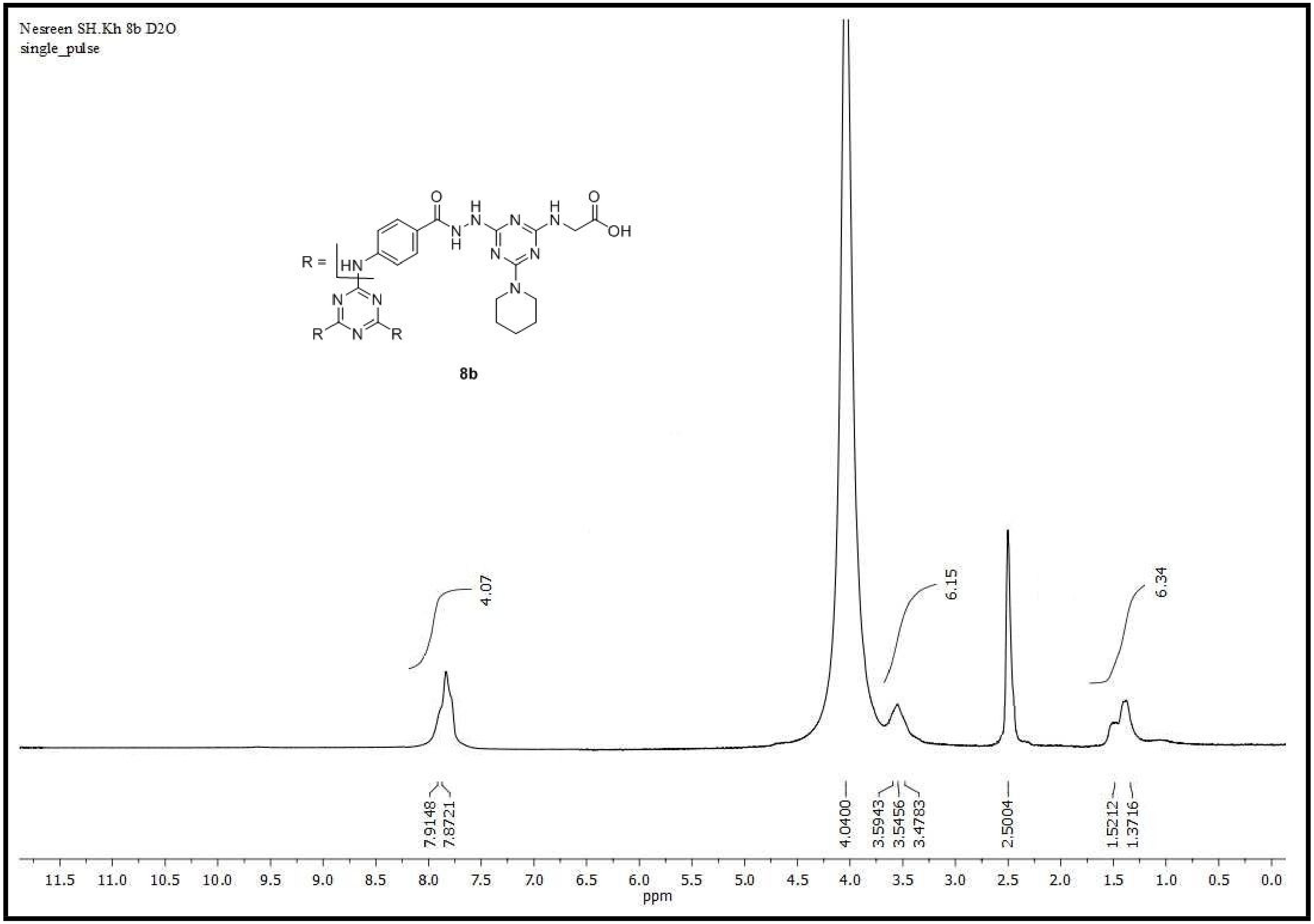

Figure S6 ^{1}H-NMR (DMSO-d_6 D_2O) spectrum of 2,2',2''-((6,6',6''-(2,2',2''-(4,4',4''-((1,3,5-triazine-2,4,6-triyl)tris(azanediyl))tris(benzoyl))tris(hydrazine-2,1- diyl))tris(4-(piperidin-1-yl)-1,3,5-triazine-6,2-diyl))tris(azanediyl))triacetic acid **8b.**

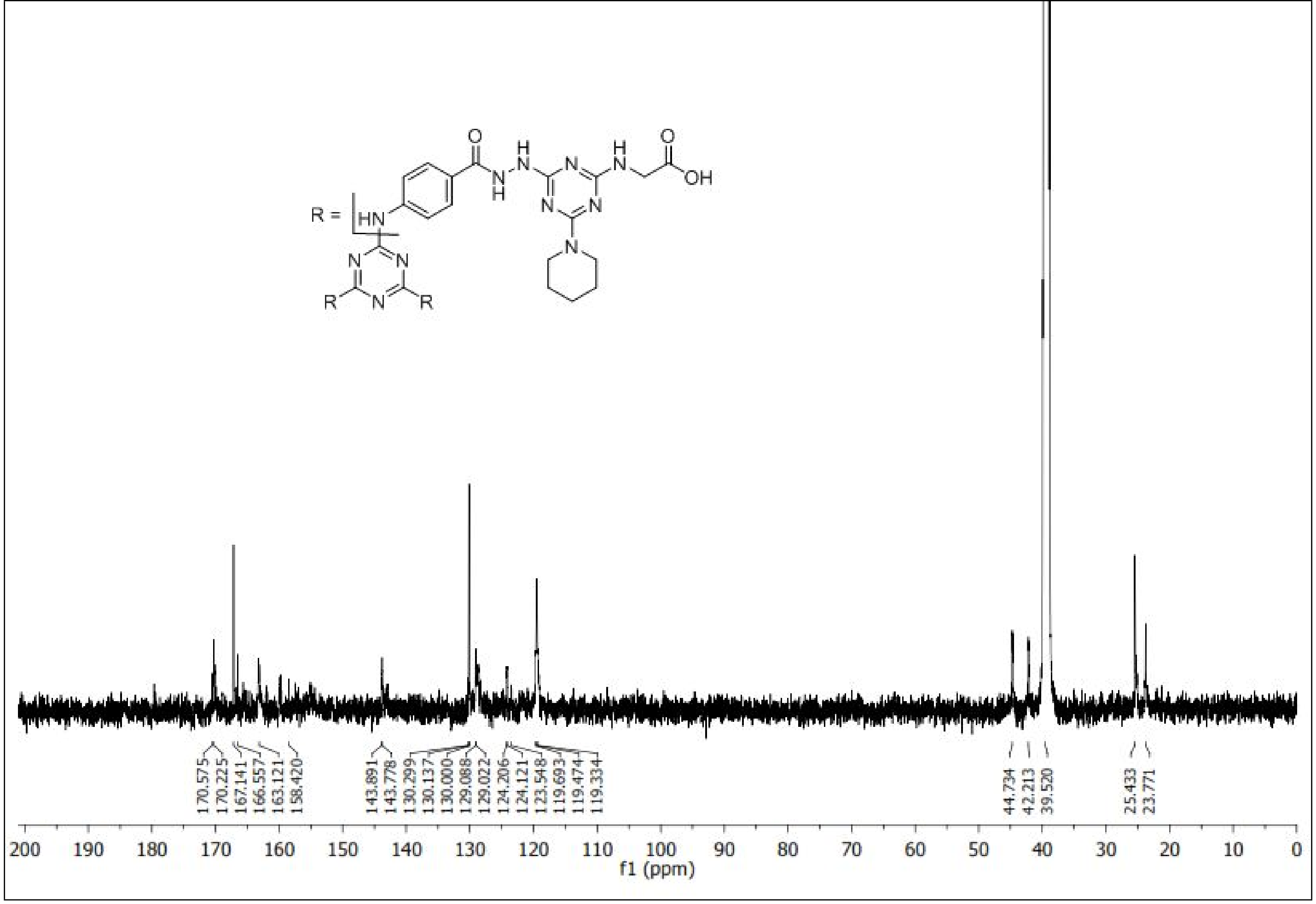

Figure S7: [13]C-NMR (DMSO-d_6) spectrum of 2,2',2''-((6,6',6''-(2,2',2''-(4,4',4''-((1,3,5-triazine-2,4,6-triyl)tris(azanediyl))tris(benzoyl))tris(hydrazine-2,1-diyl)) tris(4-(piperidin-1-yl)-1,3,5-triazine-6,2-diyl))tris(azanediyl))triacetic acid **8b.**

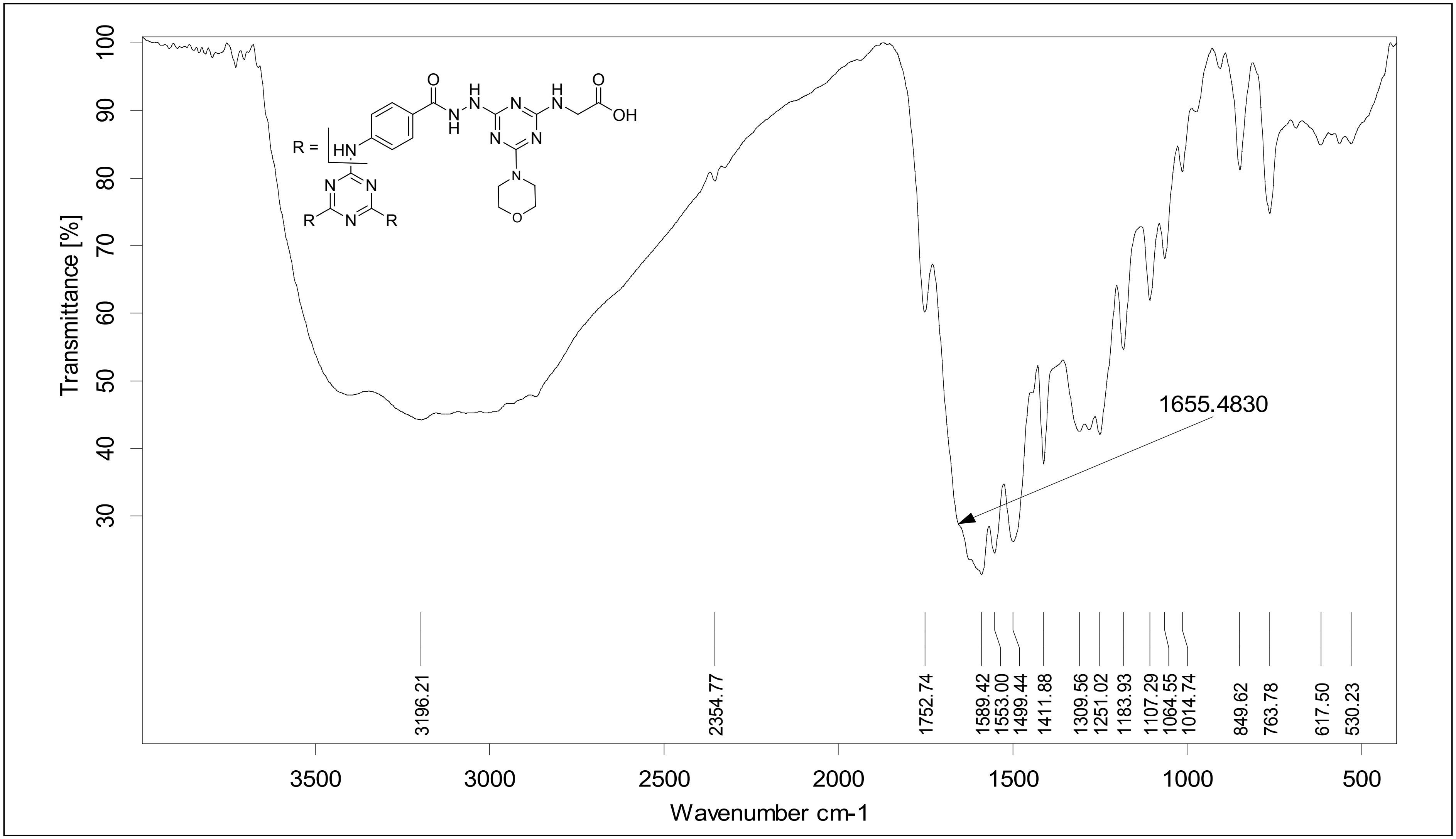

Figure S8: IR (KBr) spectrum of 2,2',2''-((6,6',6''-(2,2',2''-(4,4',4''-((1,3,5-triazine-2,4,6-triyl)tris(azanediyl))tris(benzoyl))tris(hydrazine-2,1-diyl))tris(4-morpholino-1,3,5-triazine-6,2-diyl))tris(azanediyl))triacetic acid **8c.**

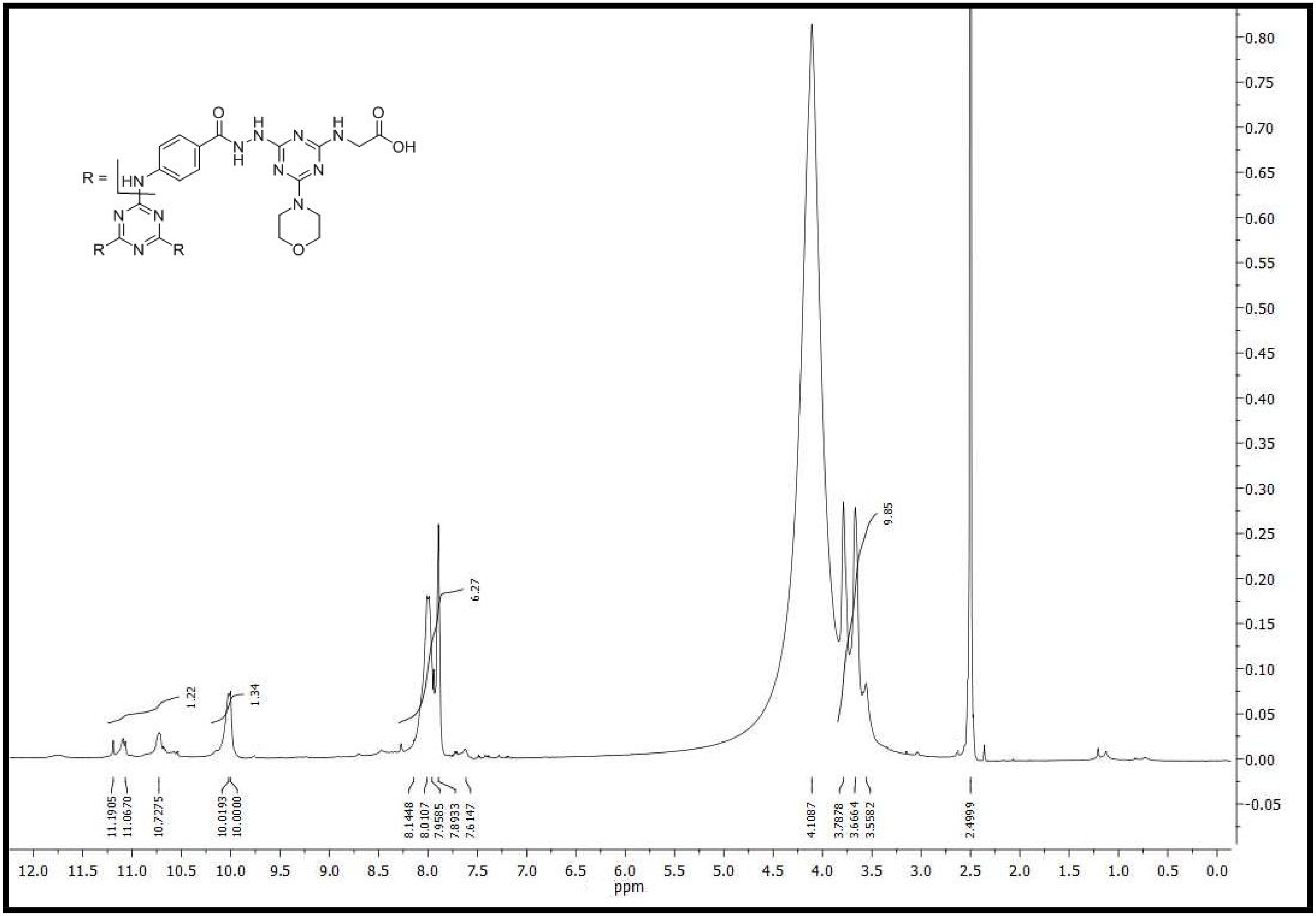

Figure 9: [1]H-NMR (DMSO-d_6) spectrum of 2,2',2''-((6,6',6''-(2,2',2''-(4,4',4''-((1,3,5-triazine-2,4,6-triyl)tris(azanediyl))tris(benzoyl))tris(hydrazine-2,1-diyl))tris(4-morpholino-1,3,5- triazine-6,2- diyl))tris(azanediyl))triacetic acid **8c.**

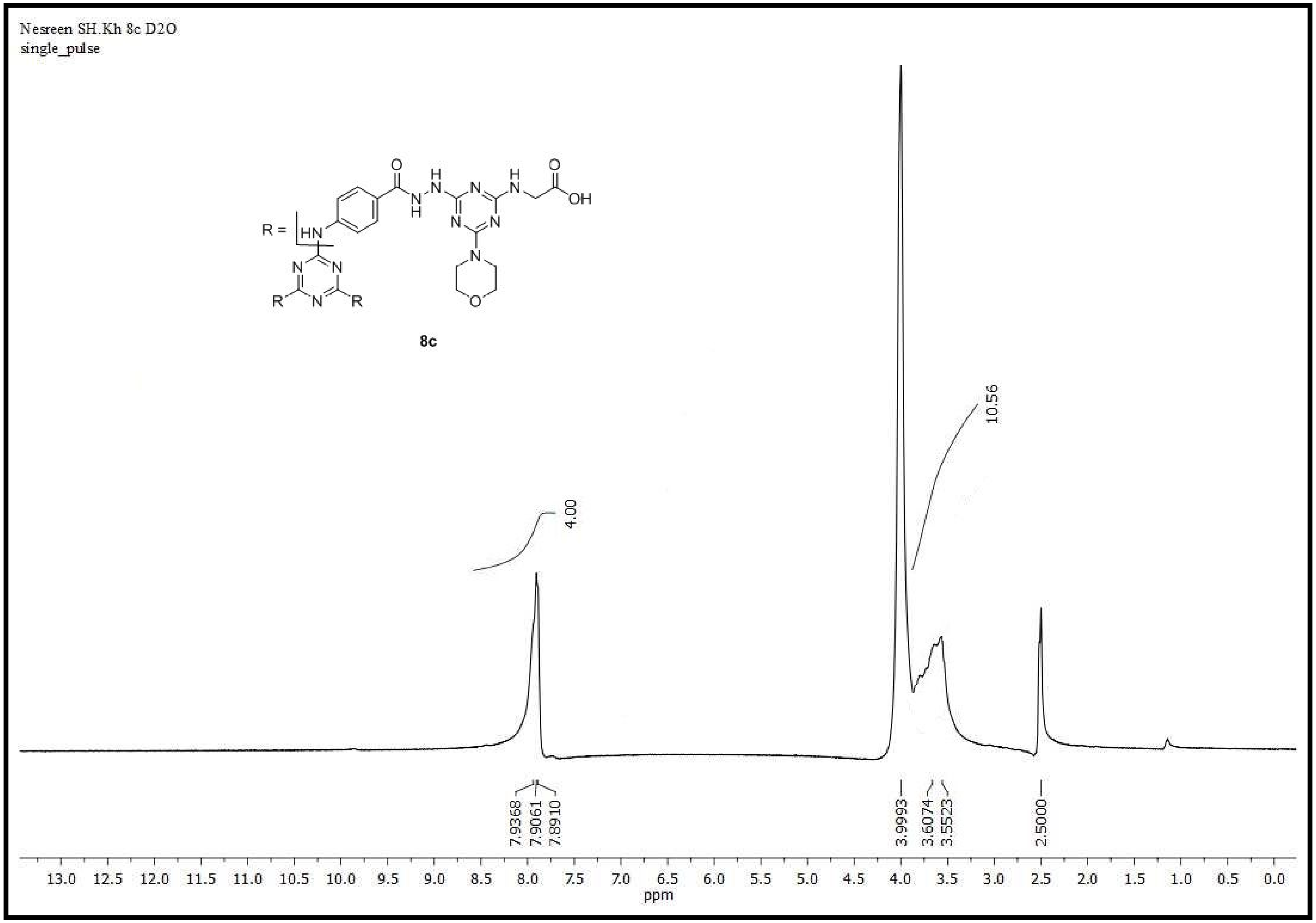

Figure S10: [1]H-NMR (DMSO-d_6, D_2O) spectrum of 2,2',2''-((6,6',6''-(2,2',2''-(4,4',4''-((1,3,5-triazine-2,4,6-triyl)tris(azanediyl))tris(benzoyl))tris(hydrazine-2,1- diyl))tris(4-morpholino-1,3,5- triazine-6,2- diyl))tris(azanediyl))triacetic acid **8c.**

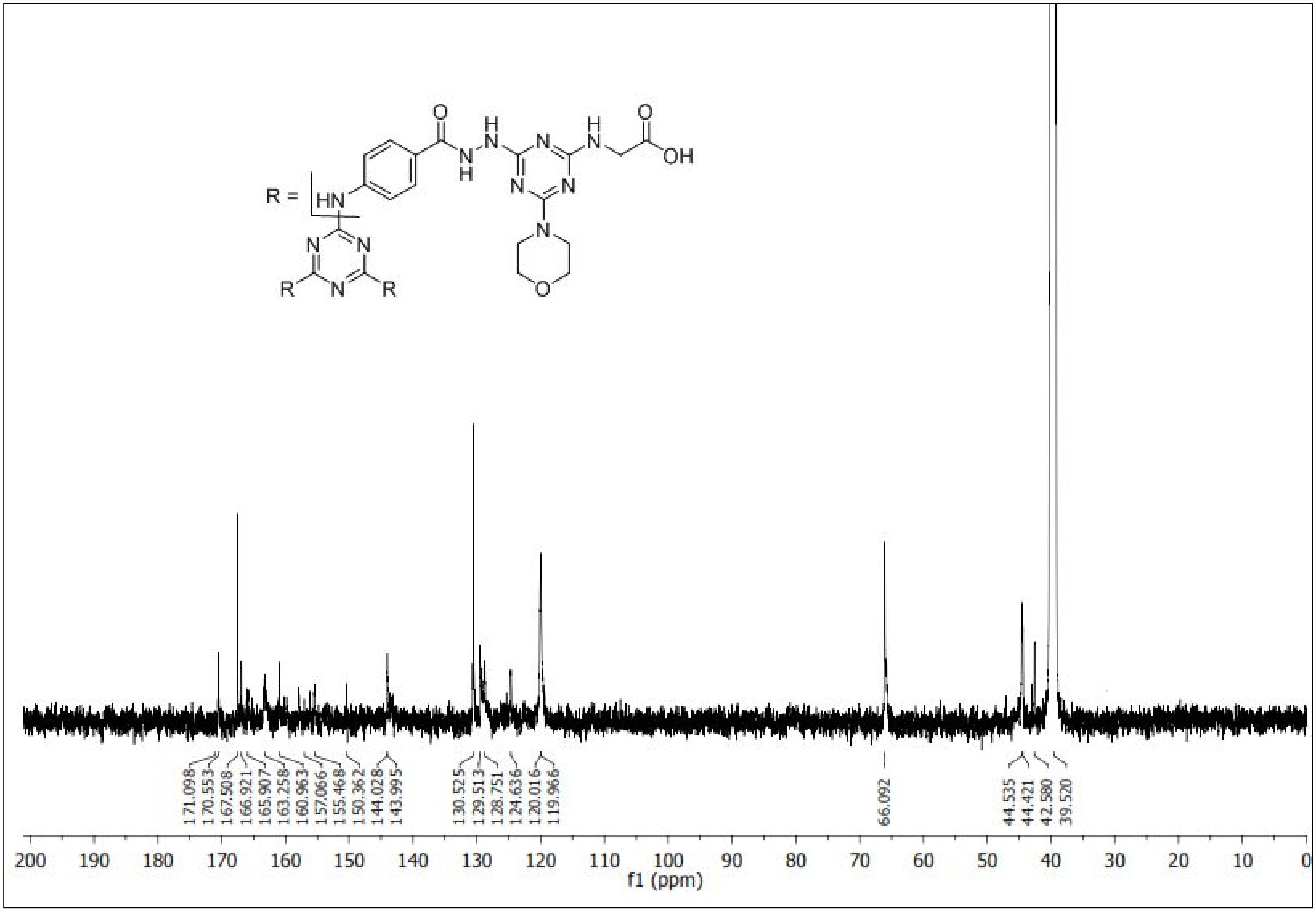

Figure S11: ^{13}C-NMR (DMSO-d_6) spectrum of 2,2',2''-((6,6',6''-(2,2',2''-(4,4',4''-((1,3,5-triazine-2,4,6-triyl)tris(azanediyl))tris(benzoyl))tris(hydrazine-2,1-diyl))tris(4-morpholino-1,3,5-triazine-6,2-diyl))tris(azanediyl))triacetic acid **8c.**

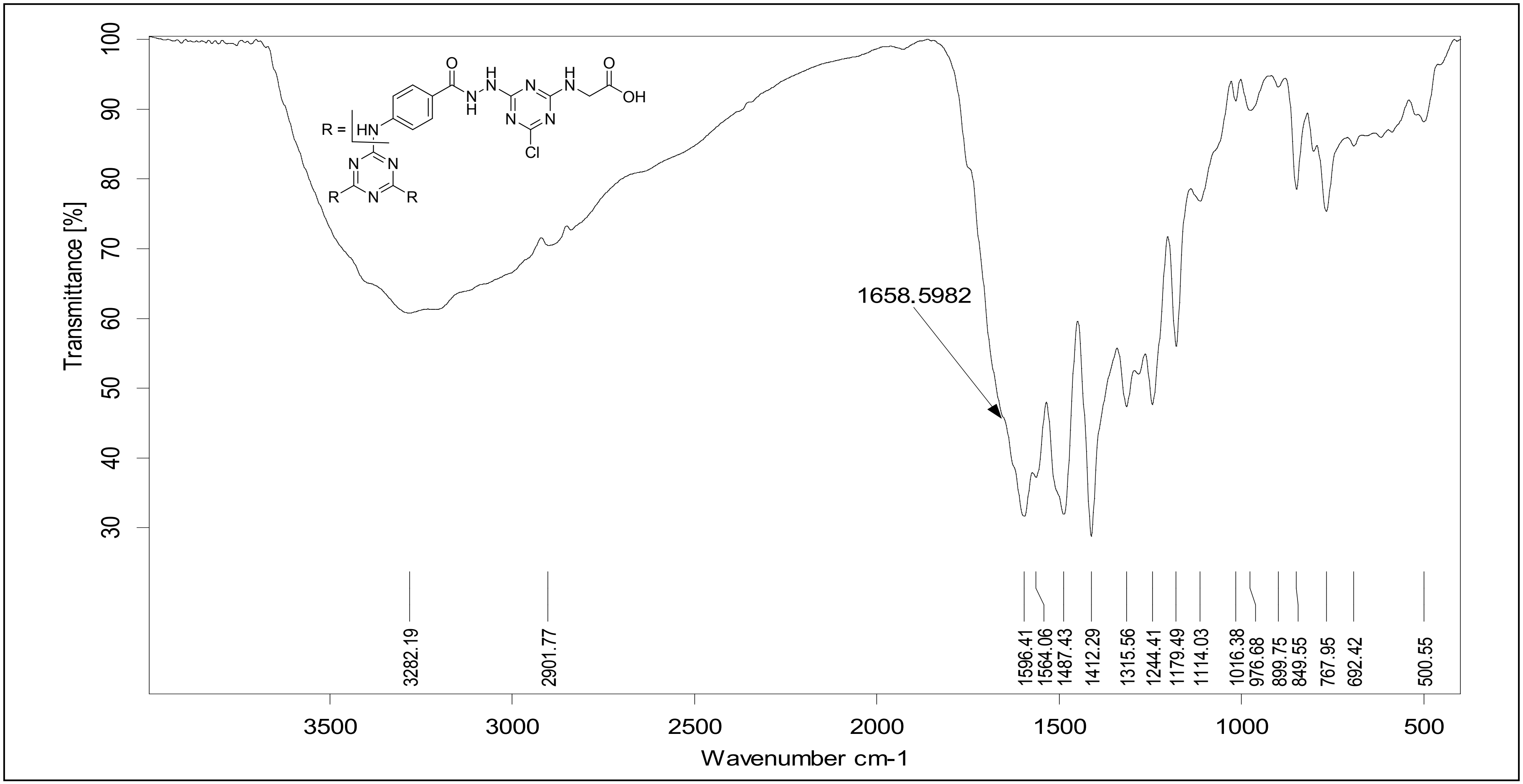

Figure S12: IR (KBr) spectrum of 2,2',2''-((6,6',6''-(2,2',2''-(4,4',4''-((1,3,5-triazine-2,4,6-triyl)tris(azanediyl))tris(benzoyl))tris(hydrazine-2,1-diyl)) tris(4-(chloro-1,3,5-triazine-6,2-diyl))tris(azanediyl))triacetic acid **10**.

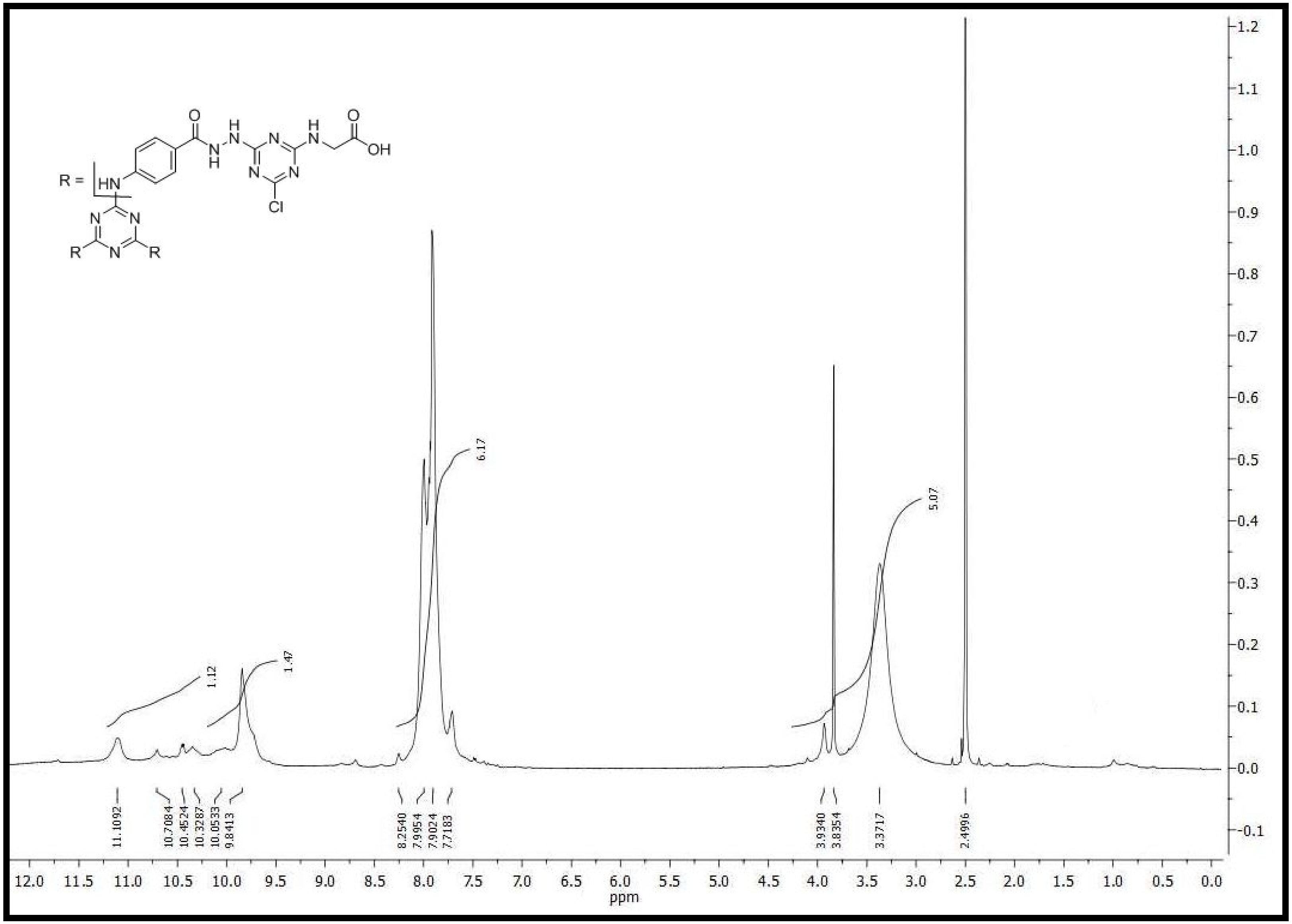

Figure S13: [1]H-NMR (DMSO-d_6) spectrum of 2,2',2''-((6,6',6''-(2,2',2''-(4,4',4''-((1,3,5-triazine-2,4,6-triyl)tris(azanediyl))tris(benzoyl))tris(hydrazine-2,1-diyl))tris(4-(chloro-1,3,5-triazine-6,2-diyl))tris(azanediyl))triacetic acid **10**.

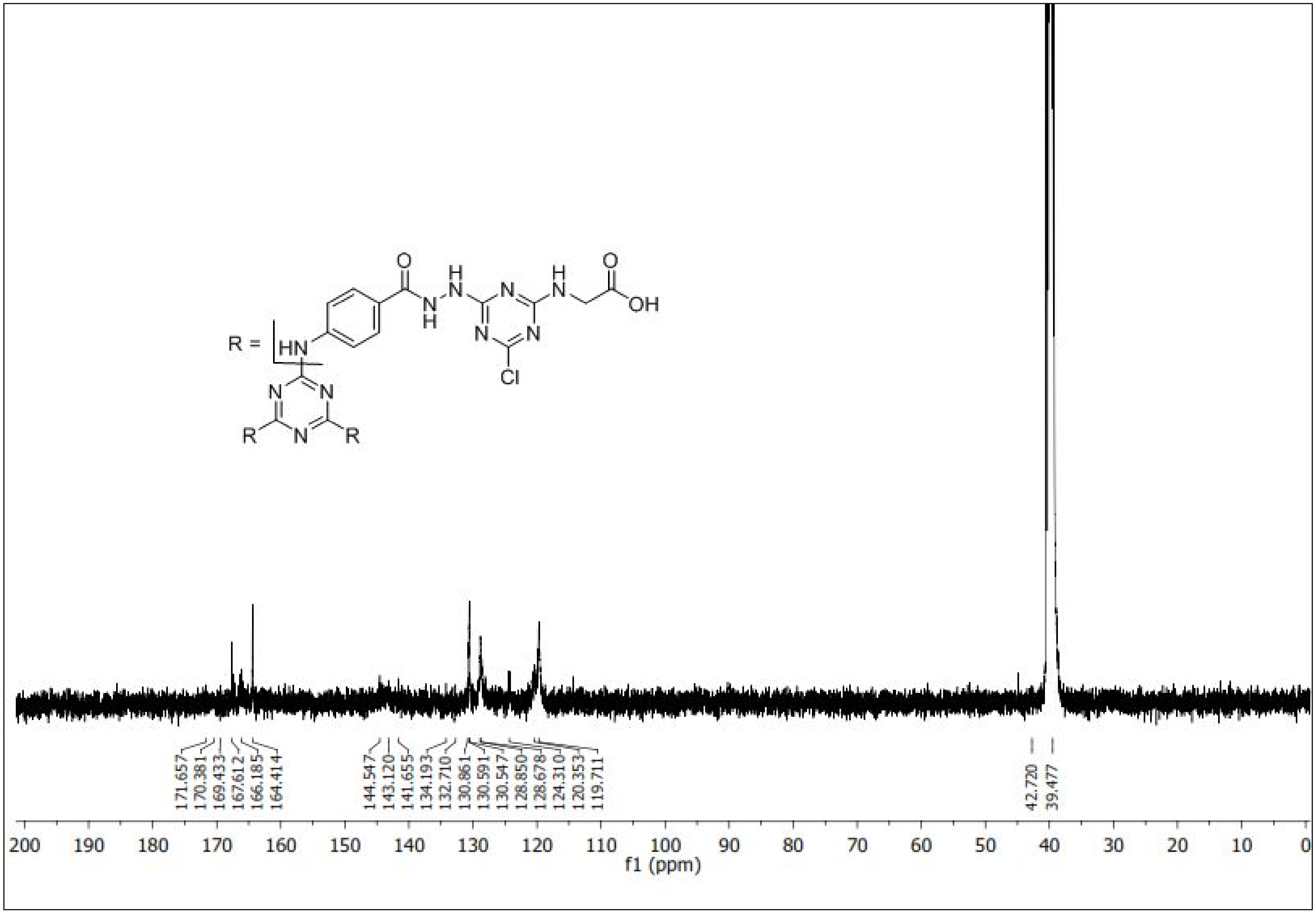

Figure S14: ^{13}C-NMR (DMSO-d_6) spectrum of 2,2',2''-((6,6',6''-(2,2',2''-(4,4',4''-((1,3,5-triazine-2,4,6-triyl)tris(azanediyl))tris(benzoyl))tris(hydrazine-2,1-diyl))tris(4-(chloro-1,3,5-triazine-6,2-diyl))tris(azanediyl))triacetic acid **10**.

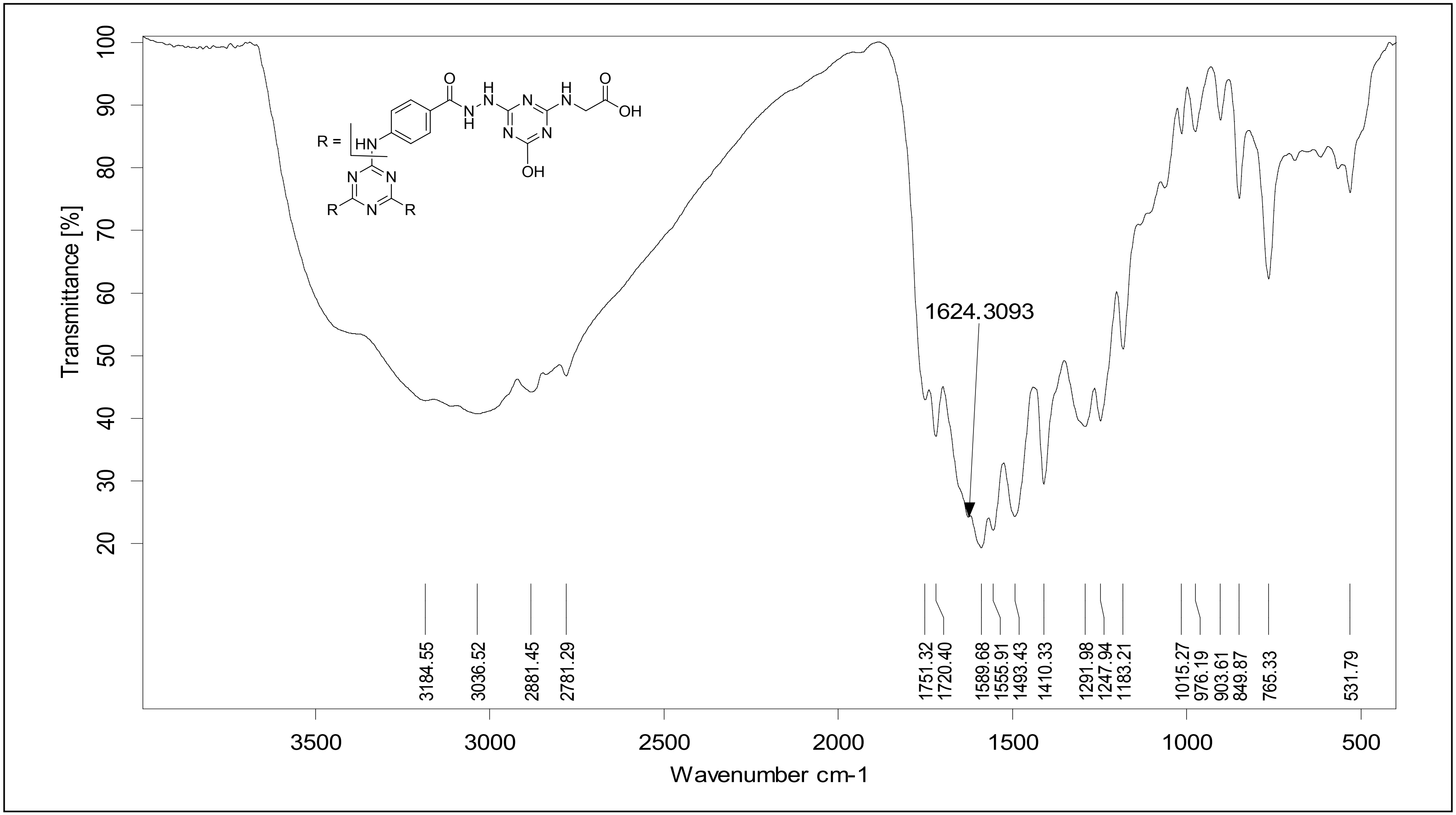

Figure S15: IR (KBr) spectrum of 2,2',2''-((6,6',6''-(2,2',2''-(4,4',4''-((1,3,5-triazine-2,4,6-triyl)tris(azanediyl))tris(benzoyl))tris(hydrazine-2,1-diyl)) tris(4-(hydroxy-1,3,5-triazine-6,2-diyl))tris(azanediyl))triacetic acid **11**.

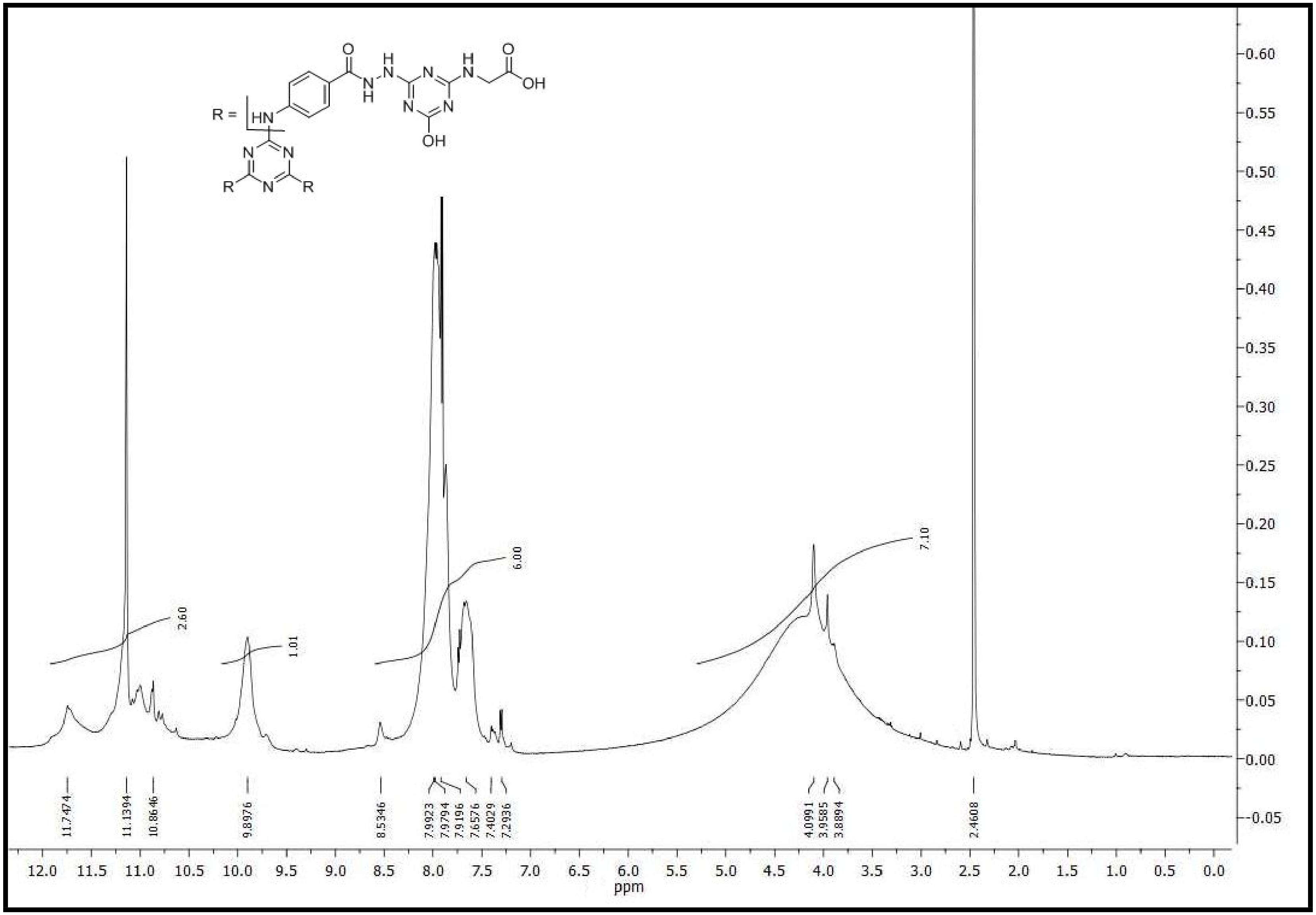

Figure S16: [1]H-NMR (DMSO-d_6) spectrum of 2,2',2''-((6,6',6''-(2,2',2''-(4,4',4''-((1,3,5-triazine-2,4,6-triyl)tris(azanediyl))tris(benzoyl))tris(hydrazine-2,1-diyl))tris(4-(hydroxy-1,3,5-triazine-6,2-diyl))tris(azanediyl))triacetic acid **11**.

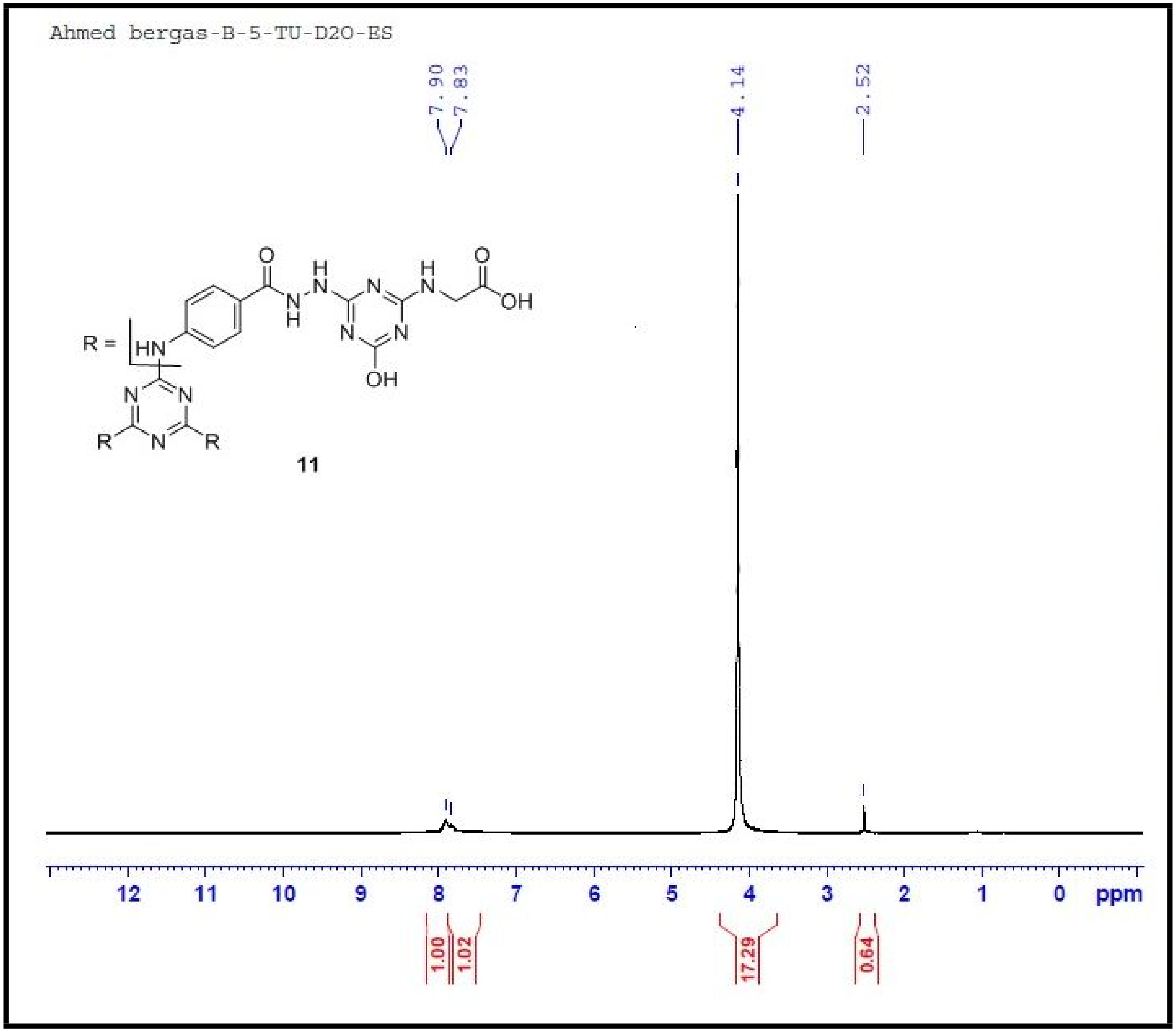

Figure S17: ^{1}H-NMR (DMSO-d_6, D_2O) spectrum of 2,2',2"-((6,6',6"-(2,2',2"-(4,4',4"-((1,3,5-triazine-2,4,6-triyl)tris(azanediyl))tris(benzoyl))tris(hydrazine-2,1- diyl))tris(4-(hydroxy-1,3,5-triazine-6,2-diyl))tris(azanediyl))triacetic acid **11**.

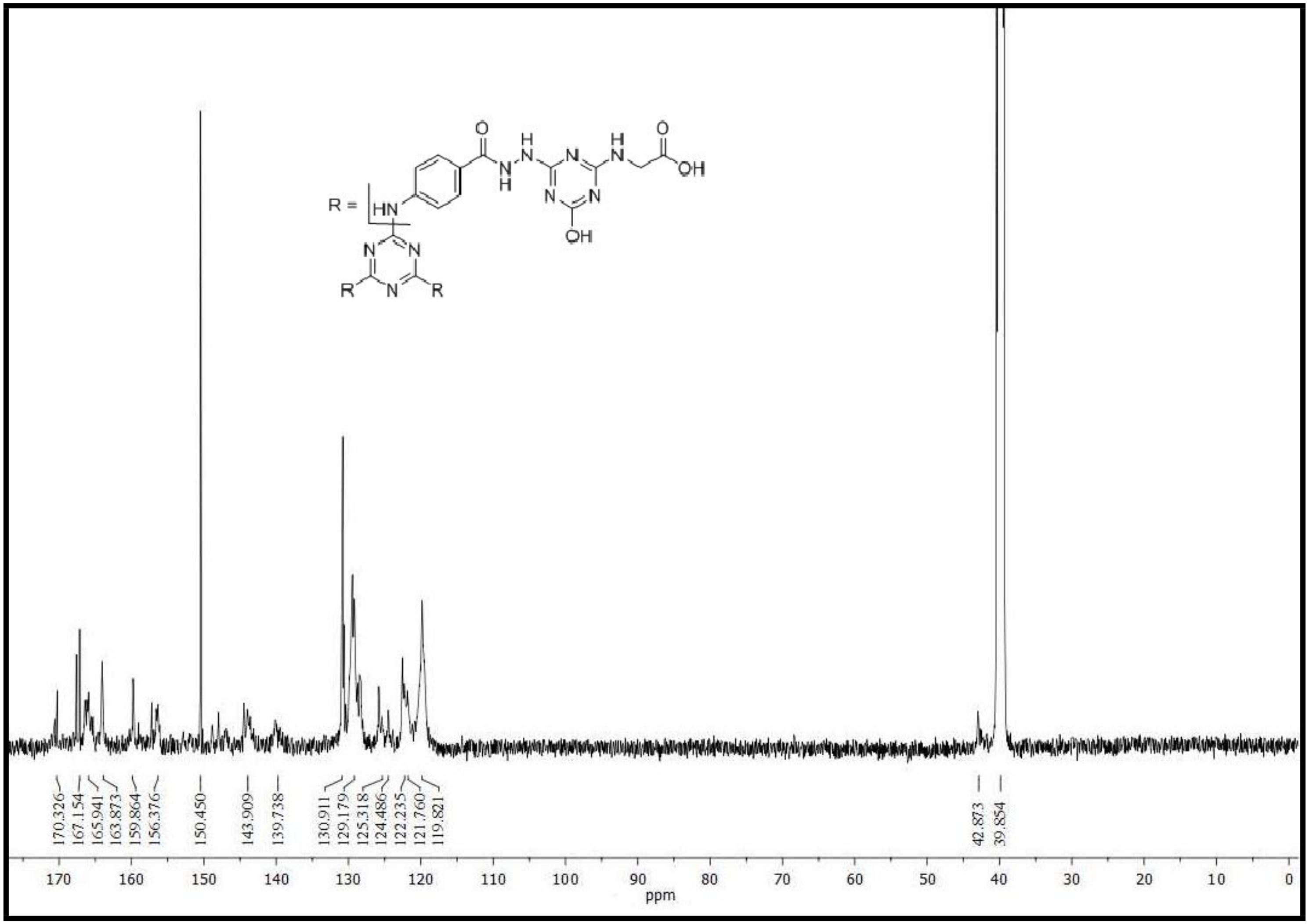

Figure S18: ^{13}C-NMR (DMSO-d_6) spectrum of 2,2',2''-((6,6',6''-(2,2',2''-(4,4',4''-((1,3,5-triazine-2,4,6-triyl)tris(azanediyl))tris(benzoyl))tris(hydrazine-2,1-diyl))tris(4-(hydroxy-1,3,5-triazine-6,2-diyl))tris(azanediyl))triacetic acid **11**.

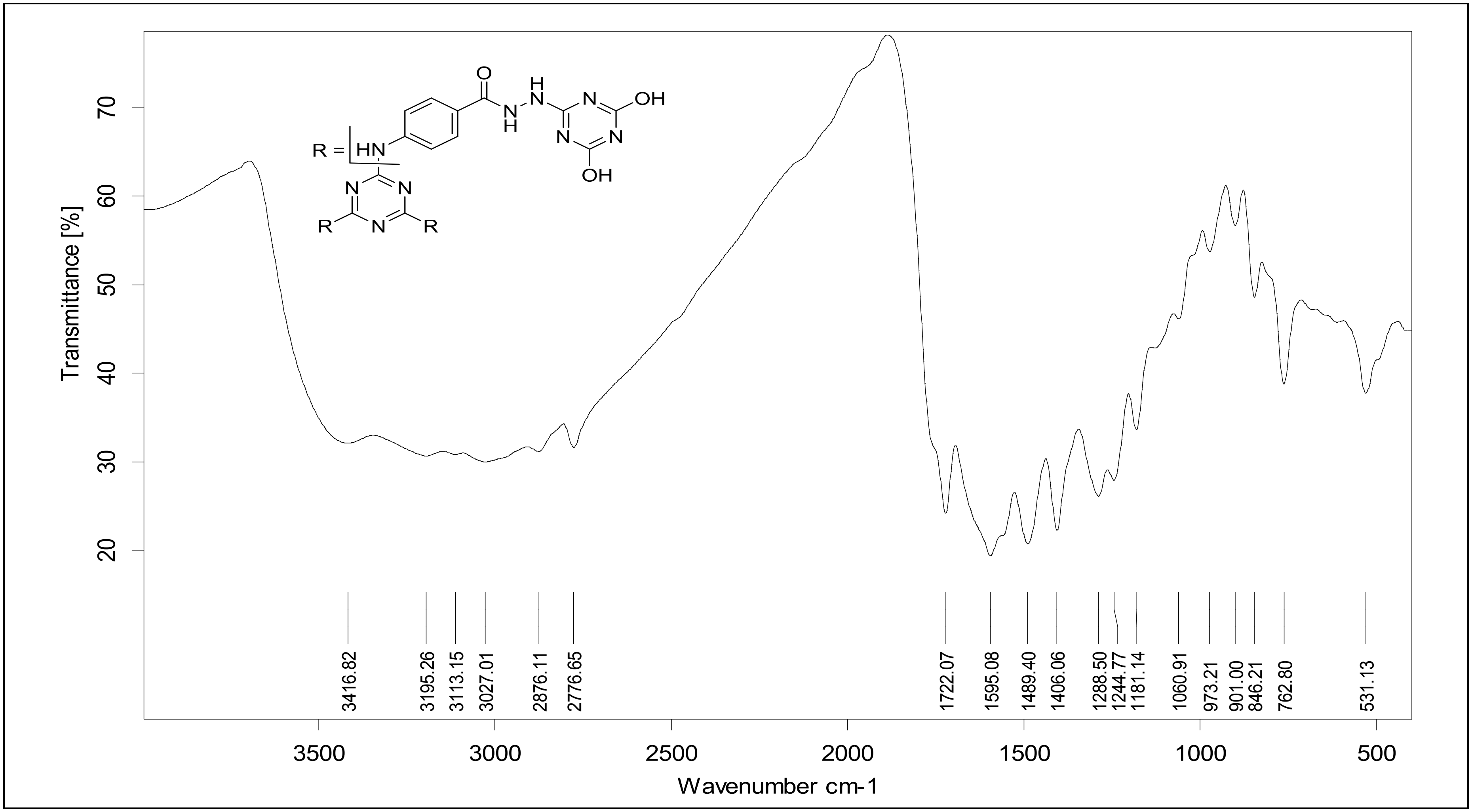

Figure S19: IR (KBr) spectrum of 4,4',4''-((1,3,5-triazine-2,4,6-triyl)tris(azanediyl))tris(*N'*-(4,6-dihydroxy-1,3,5-triazin-2-yl)benzohydrazide) **12**

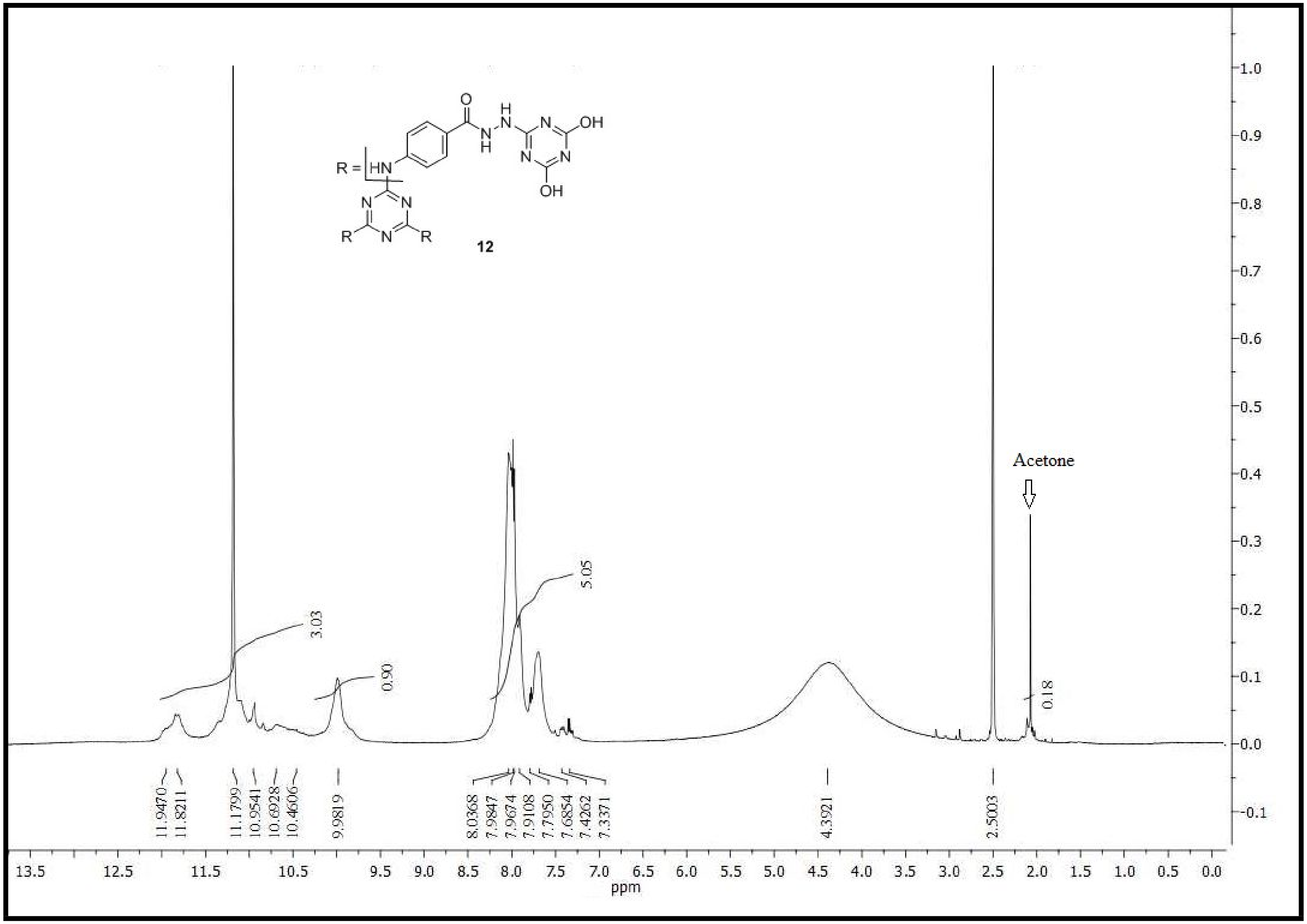

Figure S20: [1]H-NMR (DMSO-d_6) spectrum of 4,4',4''-((1,3,5-triazine-2,4,6-triyl)tris(azanediyl))tris(*N'*-(4,6-dihydroxy-1,3,5-triazin-2-yl)benzohydrazide) **12**

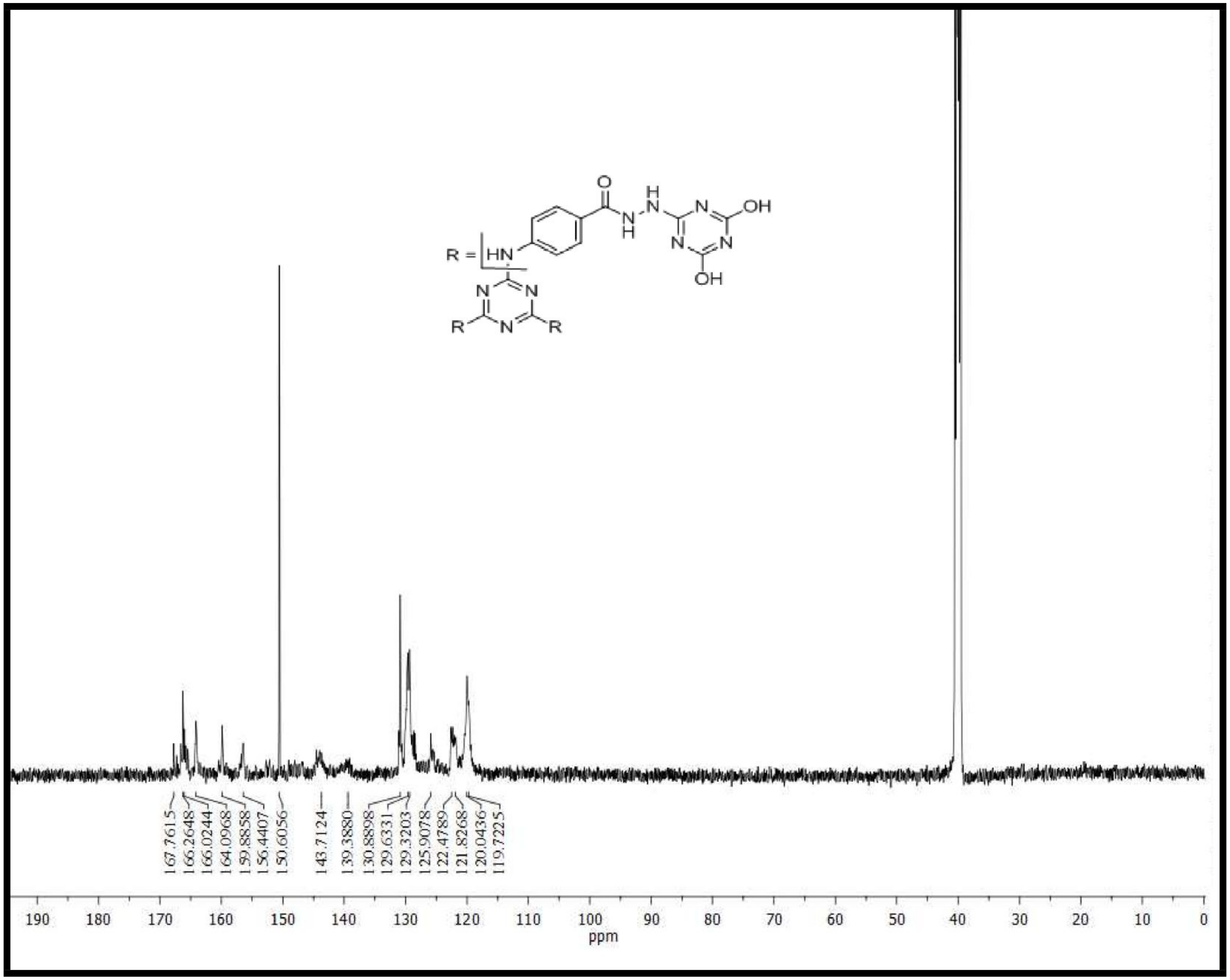

Figure S21: ^{13}C-NMR (DMSO-d_6) spectrum of 4,4',4''-((1,3,5-triazine-2,4,6-triyl)tris(azanediyl))tris(*N*'-(4,6-dihydroxy-1,3,5-triazin-2-yl)benzohydrazide)

12

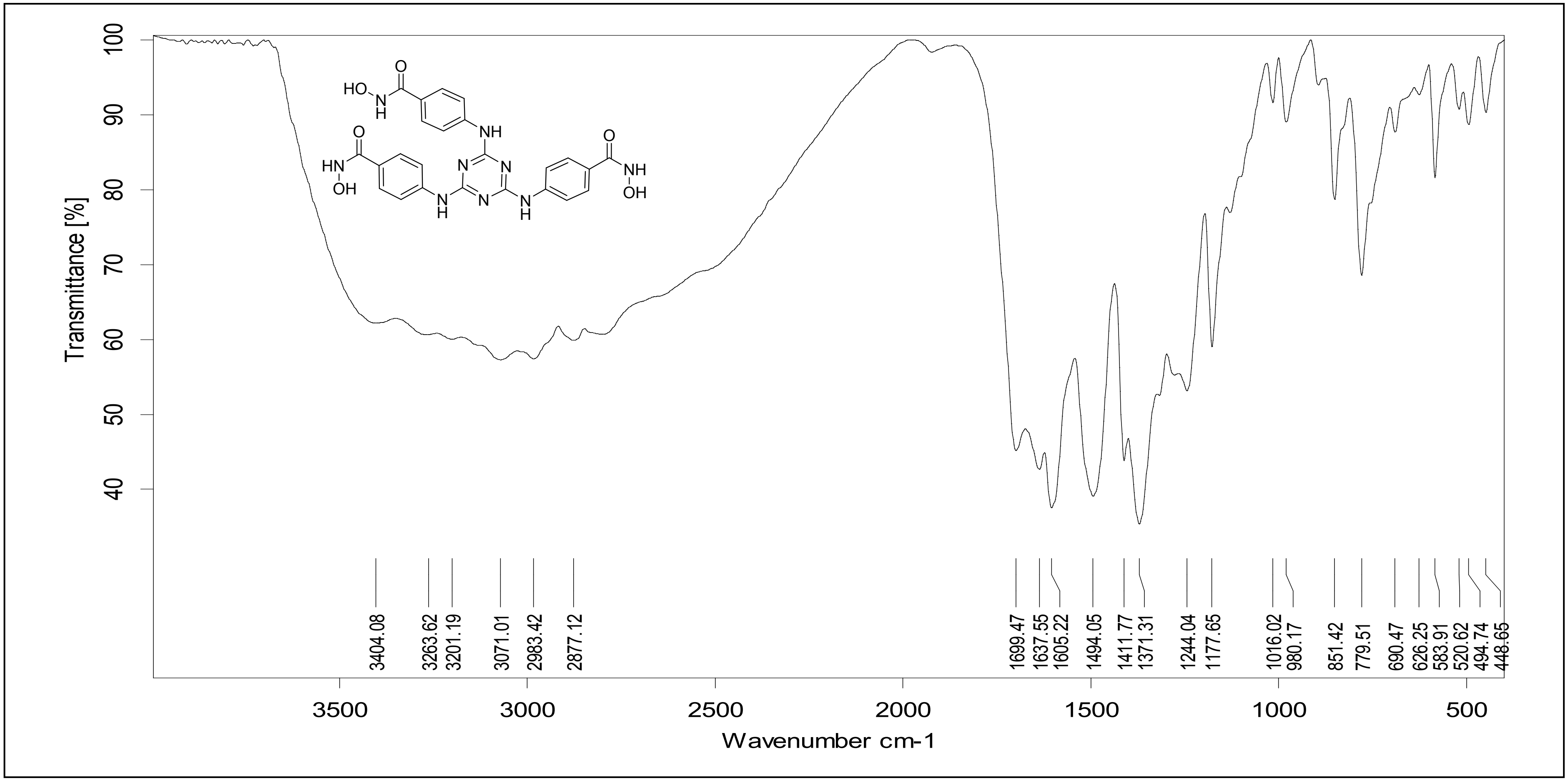

Figure S22: IR (KBr) spectrum of 4,4',4''-((1,3,5-triazine-2,4,6-triyl)tris(azanediyl))tris(*N*-hydroxybenzamide) **13**.

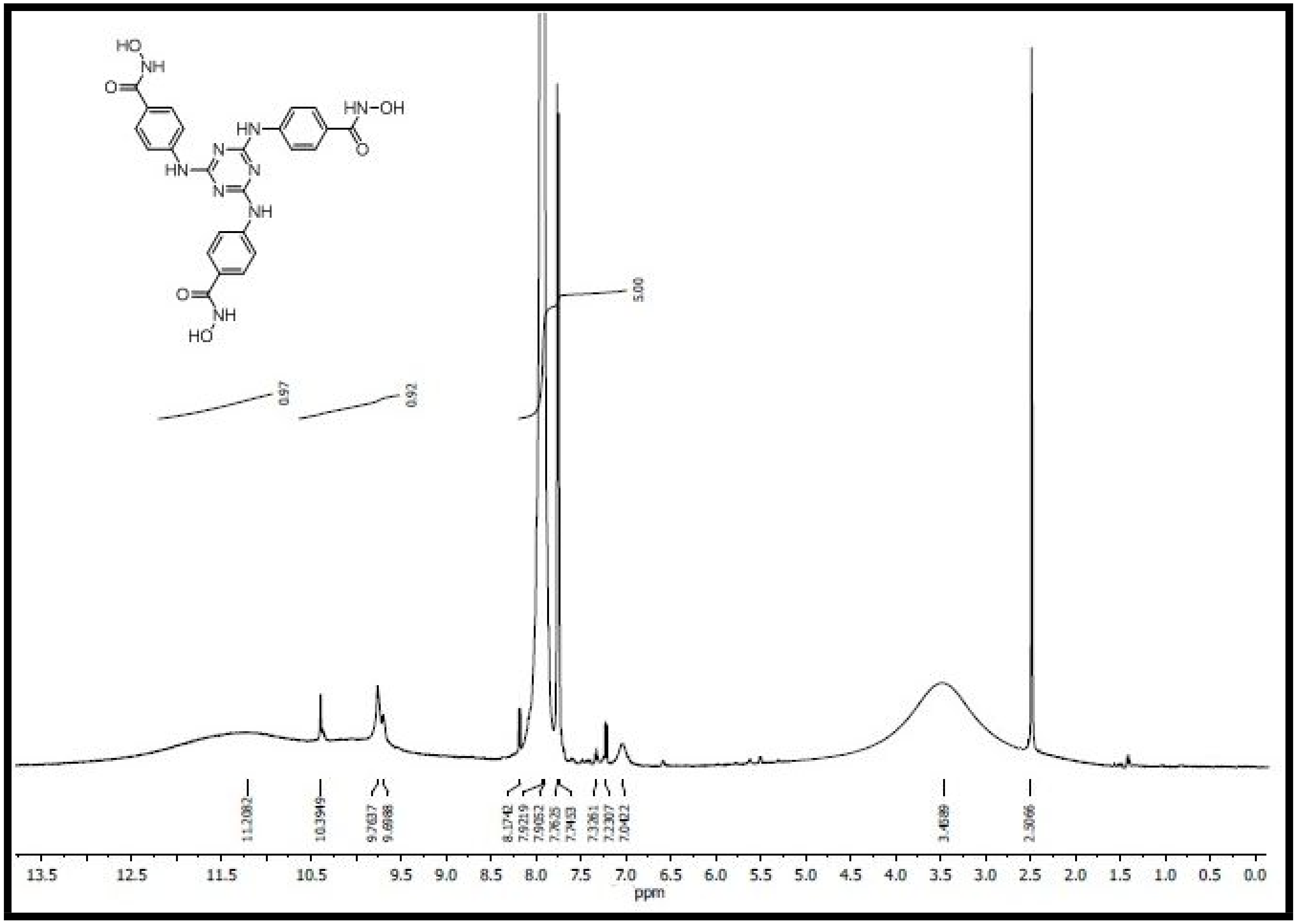

Figure S23: ^{1}H-NMR (DMSO-d_6) spectrum of 4,4',4''-((1,3,5-triazine-2,4,6-triyl)tris(azanediyl))tris(*N*-hydroxybenzamide) **13**.

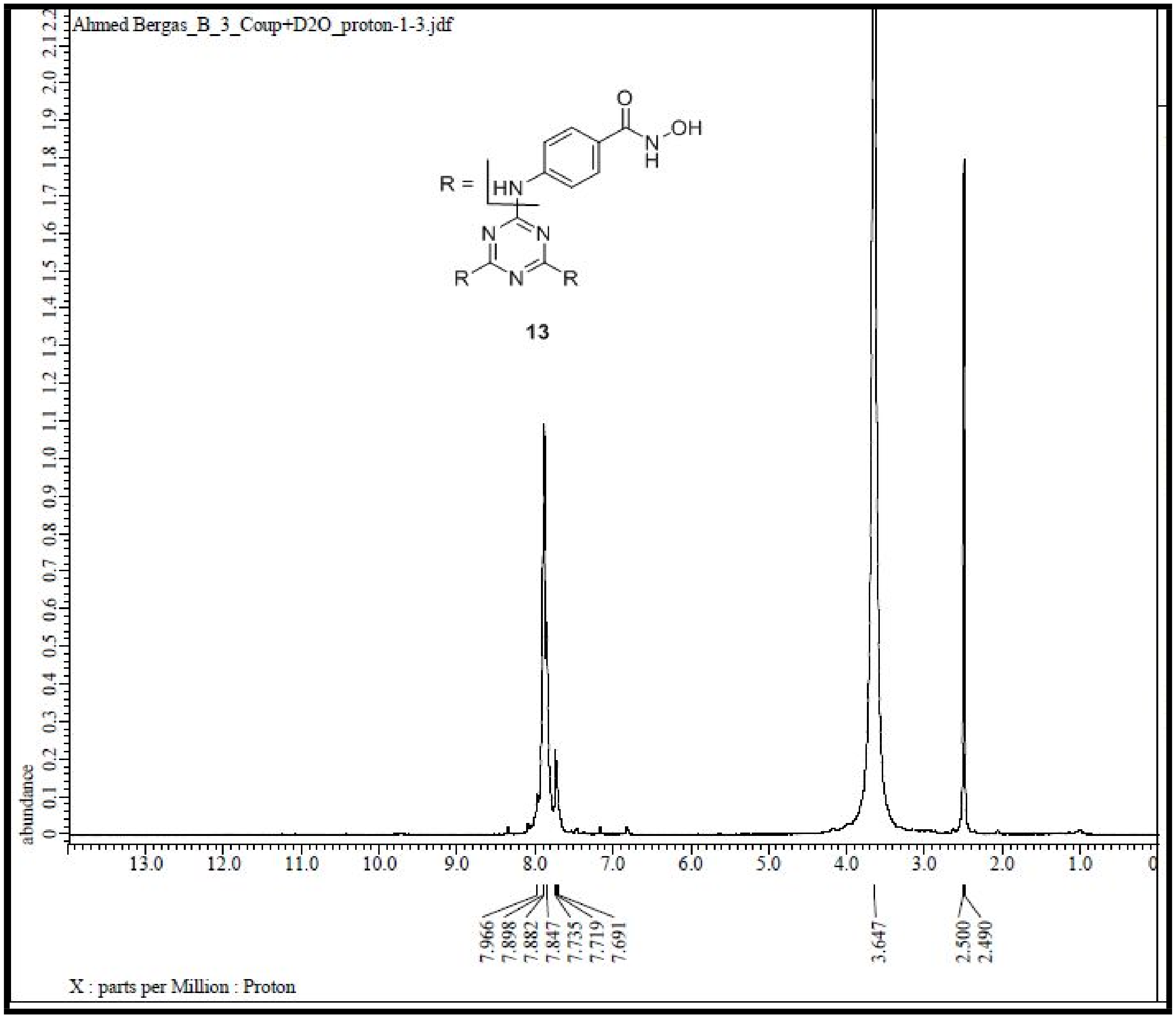

Figure S24: [1]H-NMR (DMSO-d_6, D_2O) spectrum of 4,4',4''-((1,3,5-triazine-2,4,6-triyl)tris(azanediyl))tris(*N*-hydroxybenzamide) **13**.

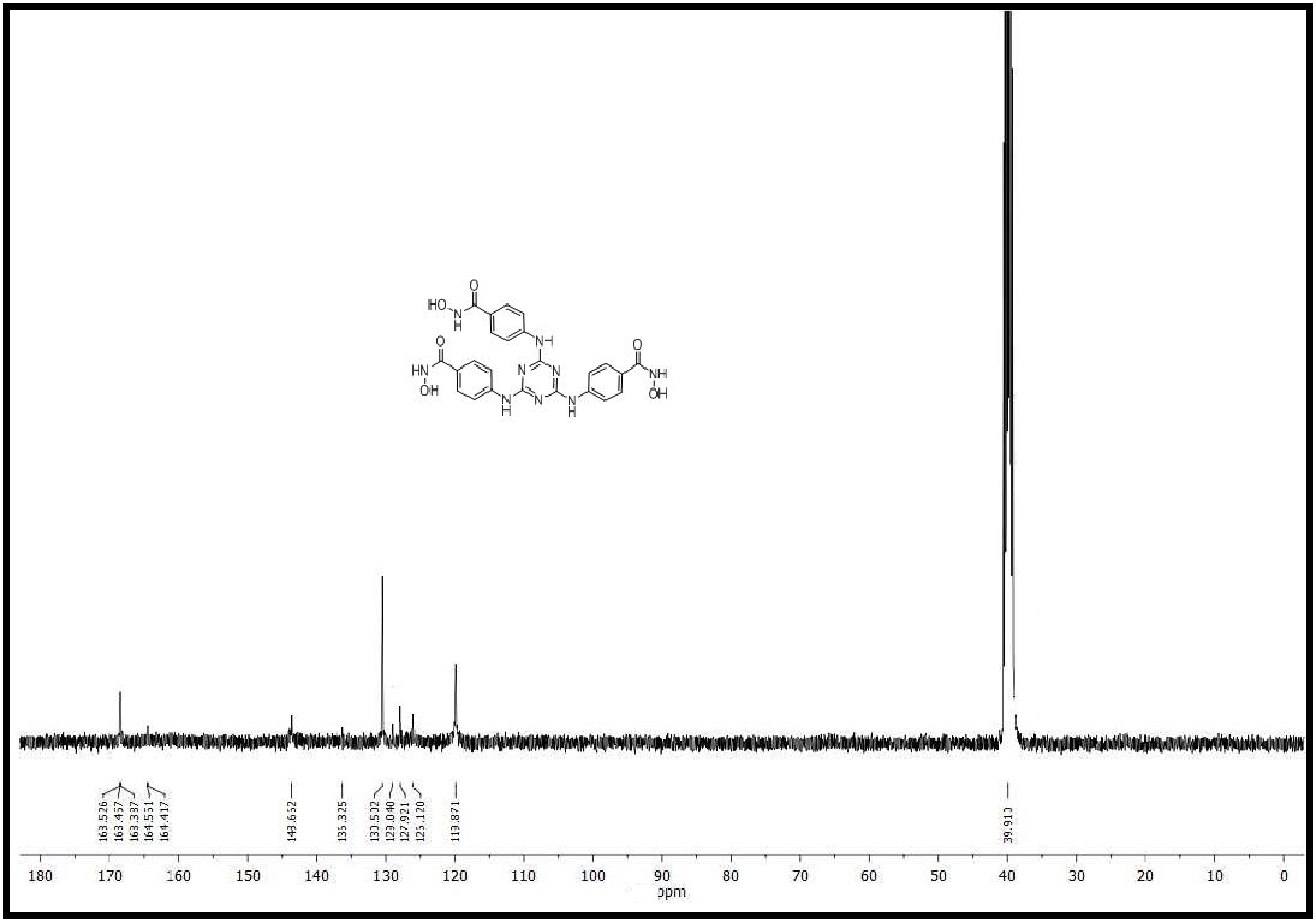

Figure S25: ^{13}C-NMR (DMSO-d_6) spectrum of 4,4',4''-((1,3,5-triazine-2,4,6-triyl)tris(azanediyl))tris(*N*-hydroxybenzamide) **13**.

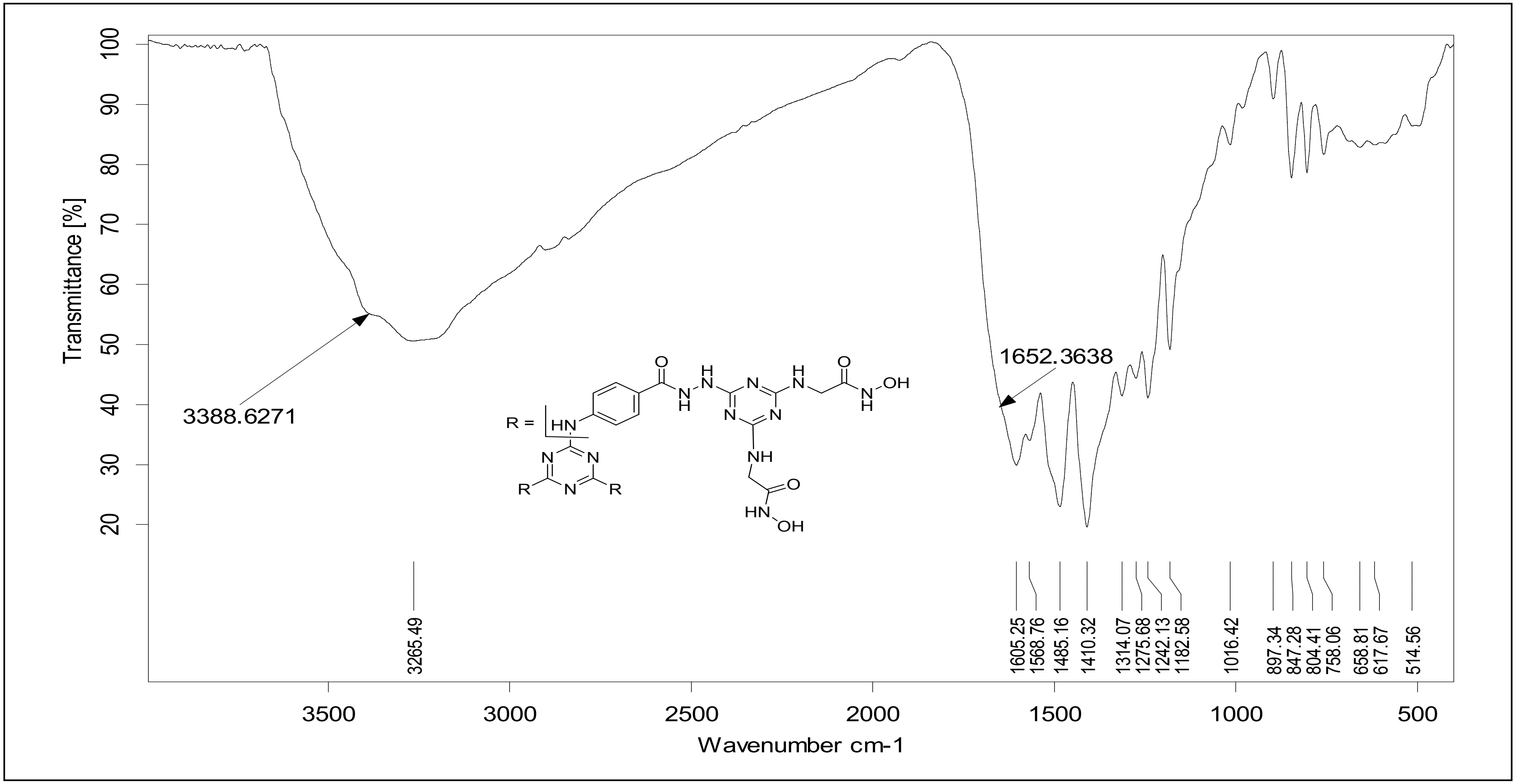

Figure S26: IR (KBr) spectrum of 2,2',2'',2''',2'''',2'''''-((6,6',6''-(2,2',2''-(4,4',4''-((1,3,5-triazine-2,4,6-triyl)tris(azanediyl))tris(benzoyl))tris(hydrazine-2,1-diyl))tris(1,3,5-triazine-6,4,2-triyl))hexakis(azanediyl))hexakis(*N*-hydroxyacetamide) **14a**.

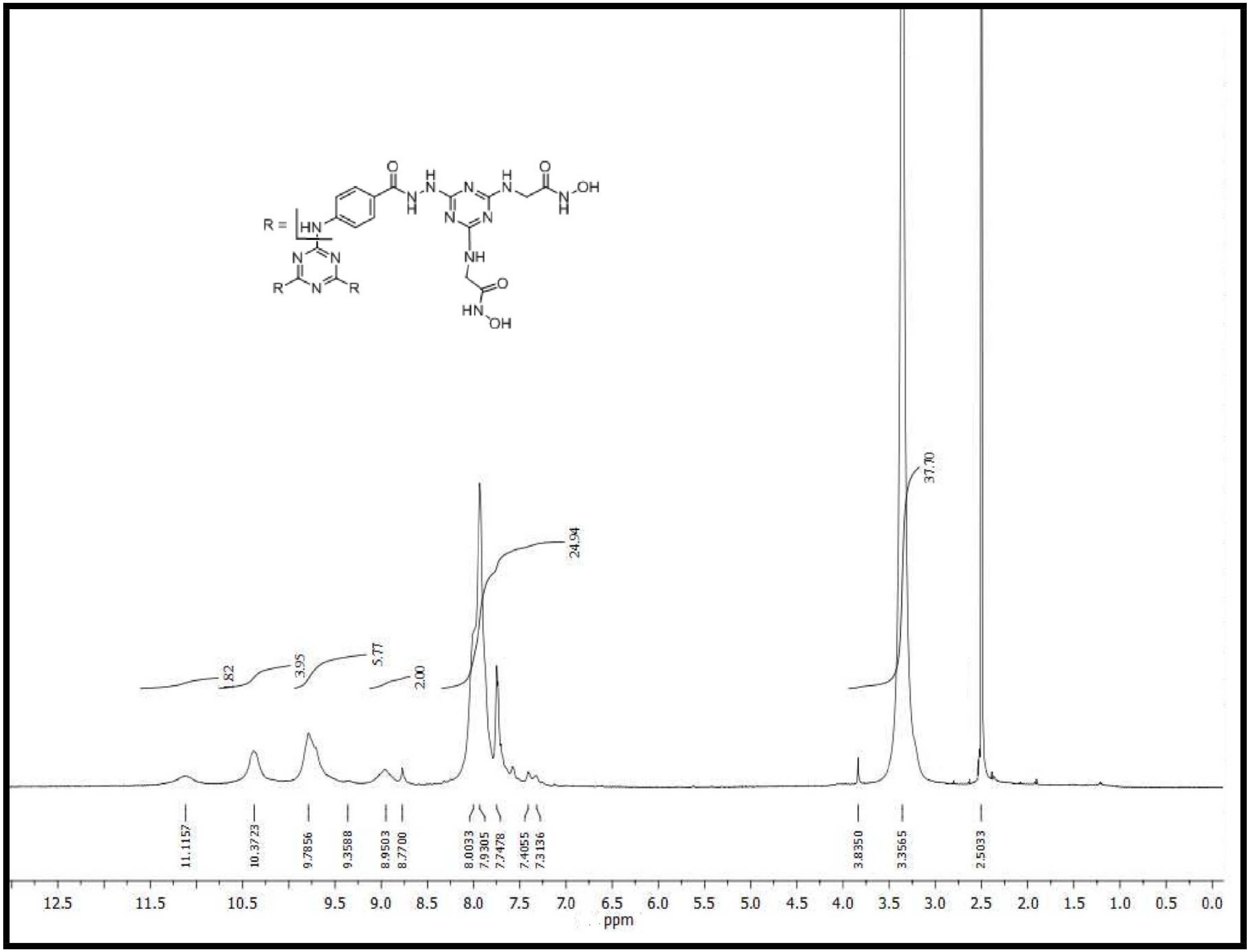

Figure S27: ^{1}H-NMR (DMSO-d_6) spectrum of 2,2',2'',2''',2'''',2'''''-((6,6',6''-(2,2',2''-(4,4',4''-((1,3,5-triazine-2,4,6-triyl)tris (azanediyl))tris(benzoyl))tris(hydrazine-2,1-diyl))tris(1,3,5-triazine-6,4,2-triyl))hexakis(azanediyl))hexakis(*N*-hydroxyacetamide) **14a**.

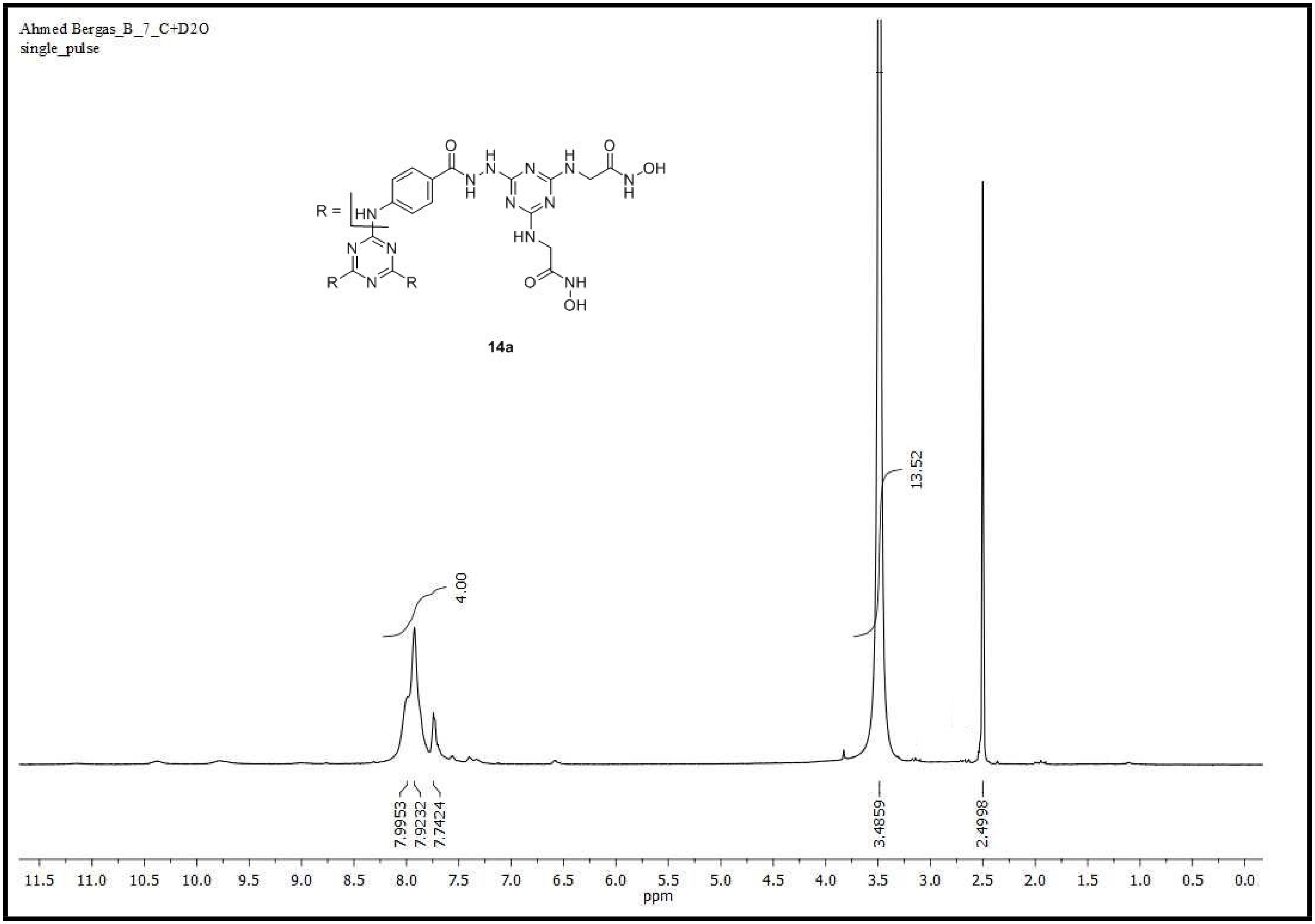

Figure S28: [1]H-NMR (DMSO-d_6, D_2O) spectrum of 2,2',2'',2''',2'''',2'''''-((6,6',6''-(2,2',2''-(4,4',4''-((1,3,5-triazine-2,4,6-triyl)tris (azanediyl))tris(benzoyl))tris(hydrazine-2,1-diyl))tris(1,3,5-triazine-6,4,2-triyl))hexakis(azanediyl))hexakis(*N*-hydroxyacetamide) **14a**.

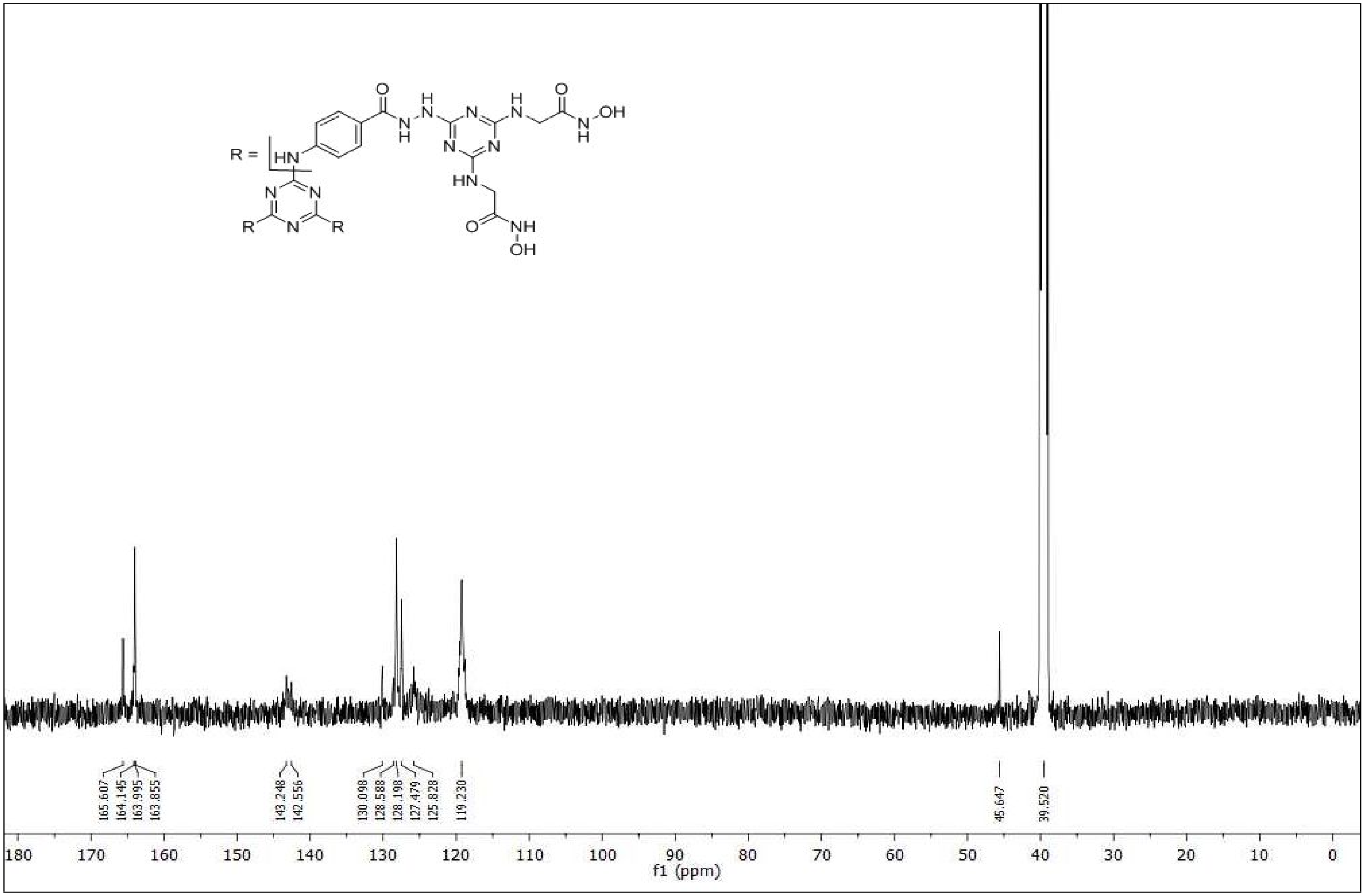

Figure S29: ^{13}C-NMR (DMSO-d_6) spectrum of 2,2',2'',2''',2'''',2'''''-((6,6',6''-(2,2',2''-(4,4',4''-((1,3,5-triazine-2,4,6-triyl)tris (azanediyl))tris(benzoyl))tris(hydrazine-2,1-diyl))tris(1,3,5-triazine-6,4,2-triyl))hexakis(azanediyl))hexakis(*N*-hydroxyacetamide) **14a**.

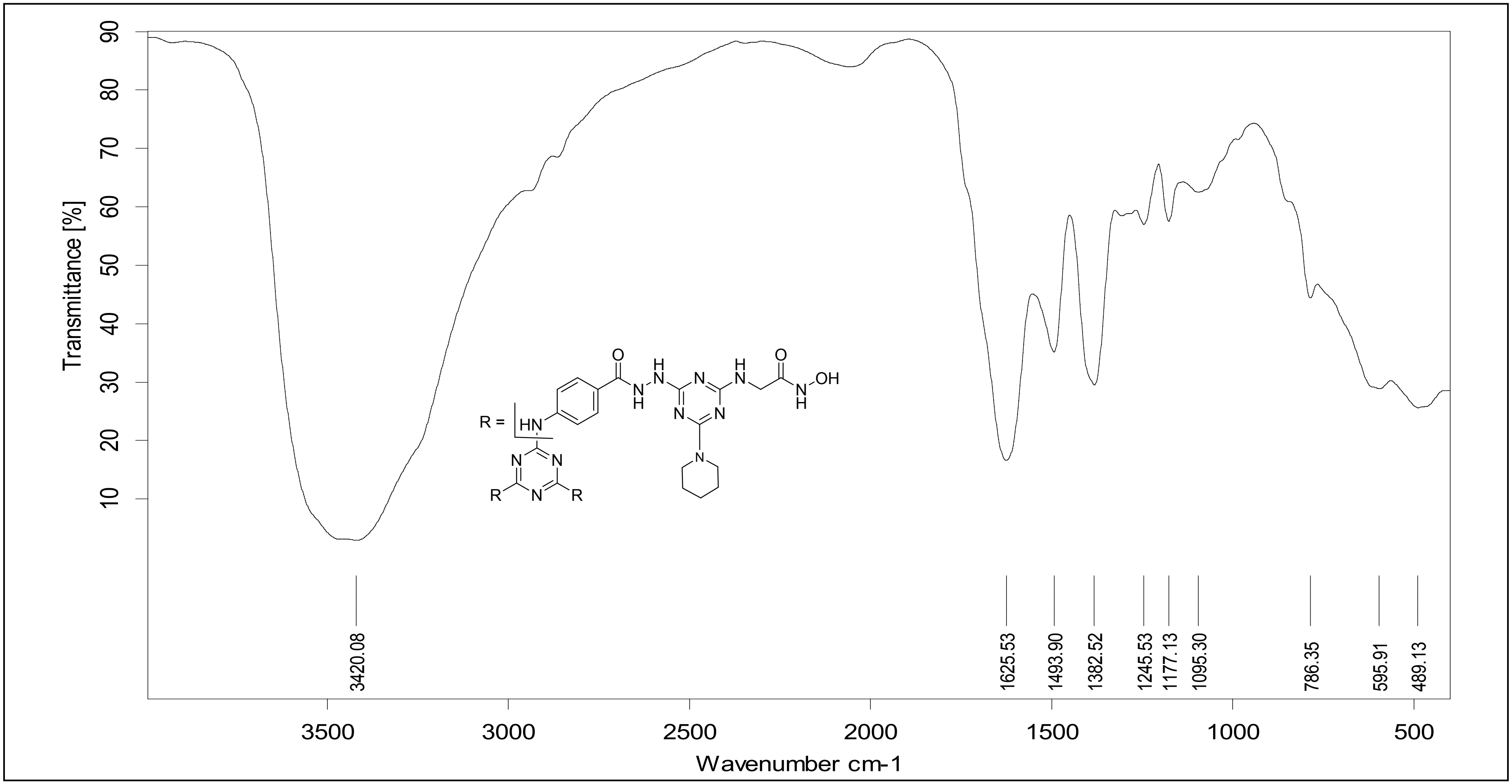

Figure S30: IR (KBr) spectrum of 2,2',2''-((6,6',6''-(2,2',2''-(4,4',4''-((1,3,5-triazine-2,4,6-triyl)tris(azanediyl))tris(benzoyl))tris(hydrazine-2,1-diyl))tris(4-(piperidin-1-yl)-1,3,5-triazine-6,2-diyl))tris(azanediyl))tris(*N*-hydroxyacetamide) **14b**.

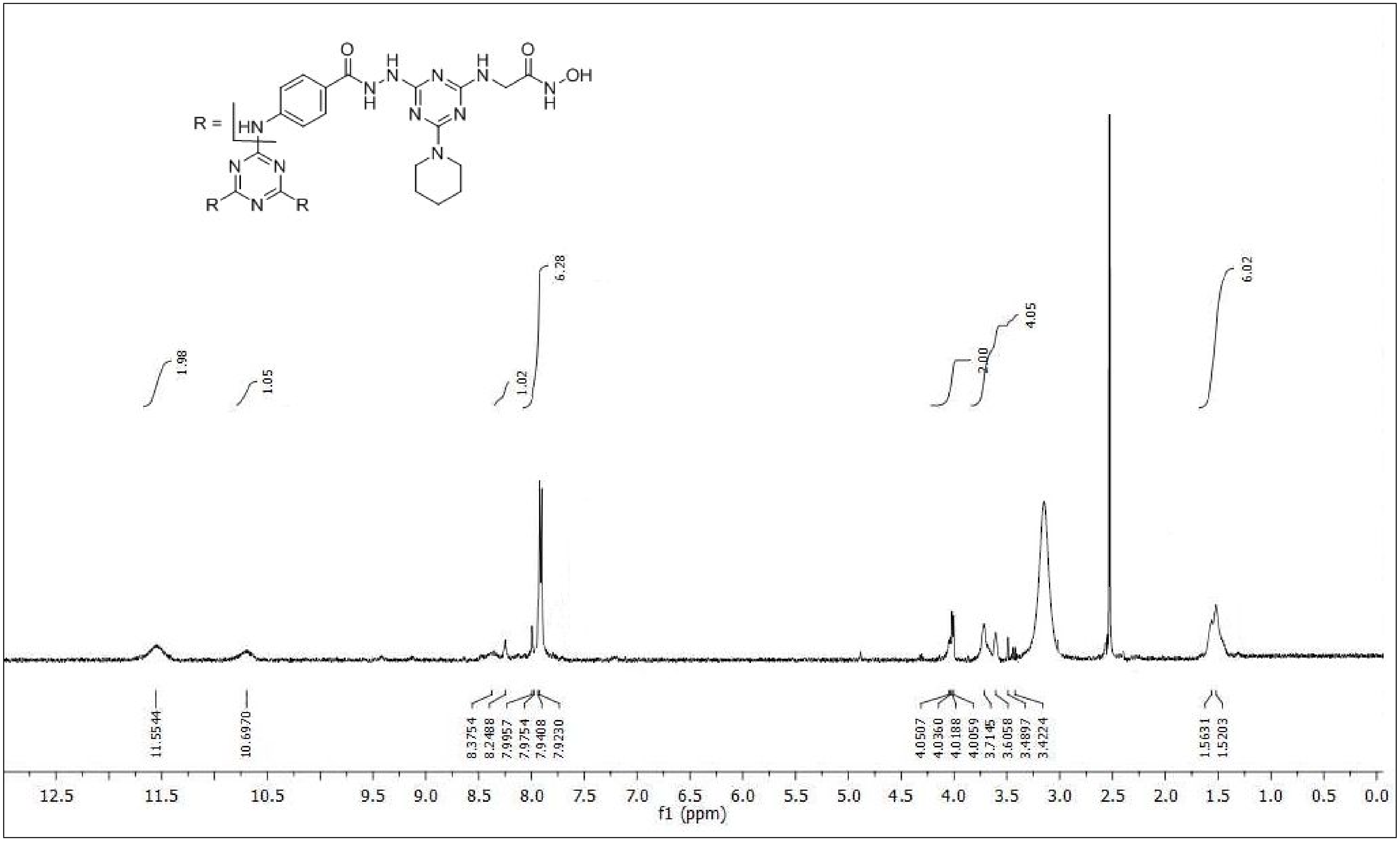

Figure S31: ^{1}H-NMR (DMSO-d_6) spectrum of 2,2',2''-((6,6',6''-(2,2',2''-(4,4',4''-((1,3,5-triazine-2,4,6-triyl)tris(azanediyl))tris(benzoyl))tris(hydrazine-2,1-diyl))tris (4-(piperidin-1-yl)-1,3,5-triazine-6,2-diyl))tris(azanediyl))tris(*N*-hydroxyacetamide) **14b**.

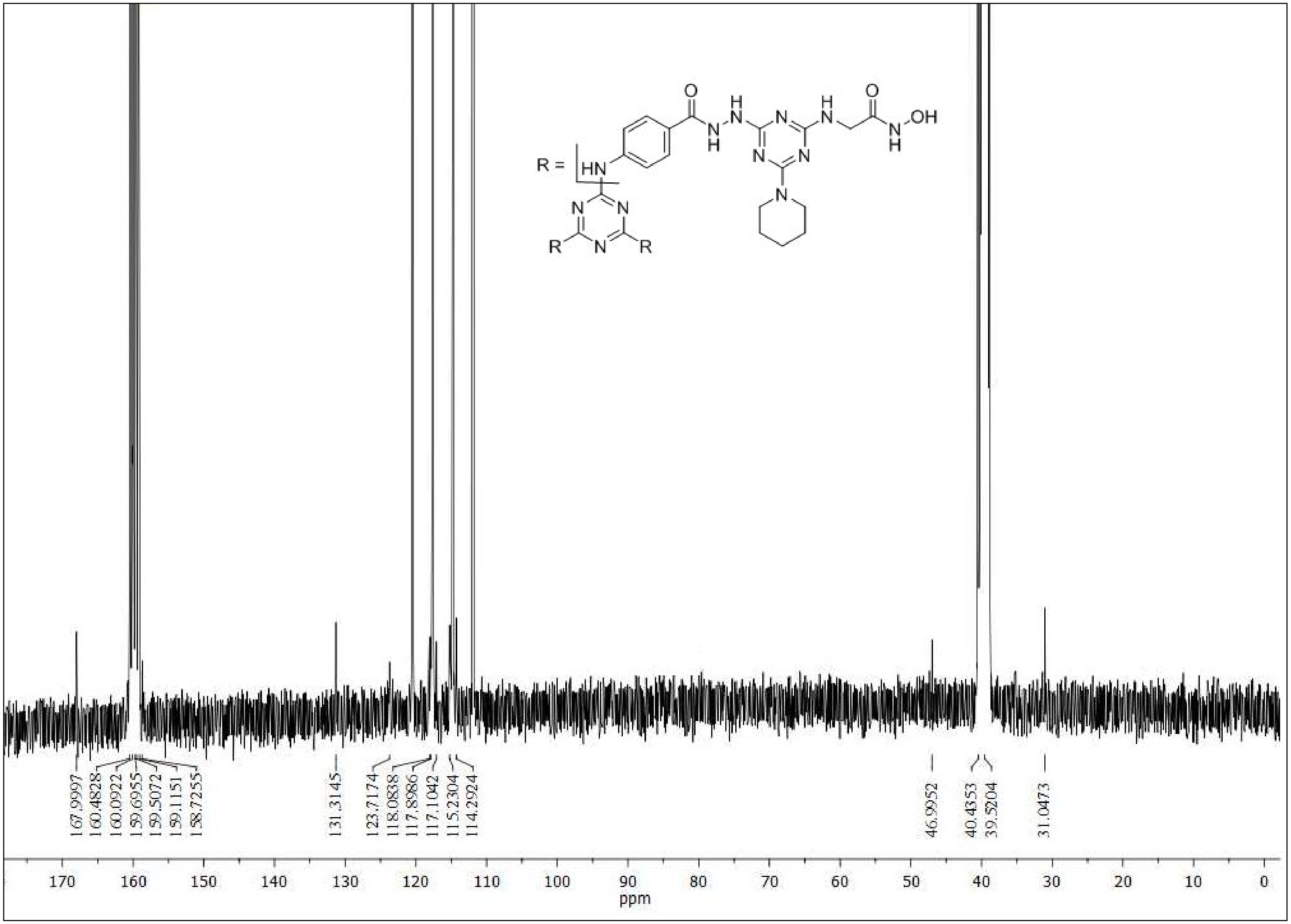

Figure S32: ^{13}C-NMR (DMSO-d_6, TFA) spectrum of 2,2',2''-((6,6',6''-(2,2',2''-(4,4',4''-((1,3,5-triazine-2,4,6-triyl)tris(azanediyl))tris(benzoyl))tris(hydrazine-2,1- diyl))tris(4-(piperidin-1-yl)-1,3,5-triazine-6,2-diyl))tris(azanediyl))tris (*N*-hydroxyacetamide) **14b.**

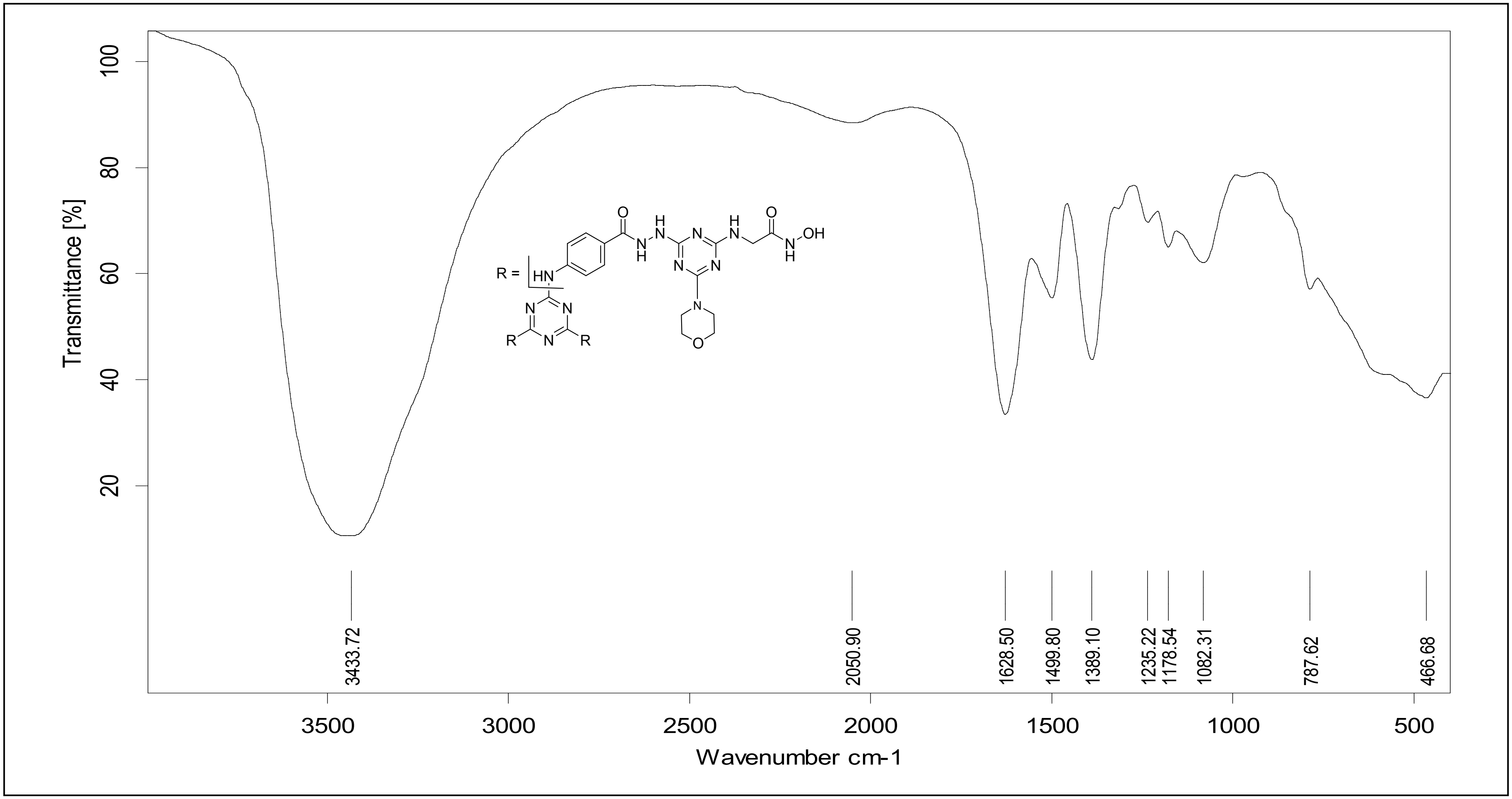

Figure S33: IR (KBr) spectrum of 2,2',2''-((6,6',6''-(2,2',2''-(4,4',4''-((1,3,5-triazine-2,4,6-triyl)tris(azanediyl))tris(benzoyl))tris(hydrazine-2,1-diyl))tris(4-(morpholin-4-yl)-1,3,5-triazine-6,2-diyl))tris(azanediyl))tris(*N*-hydroxyacetamide) **14c**.

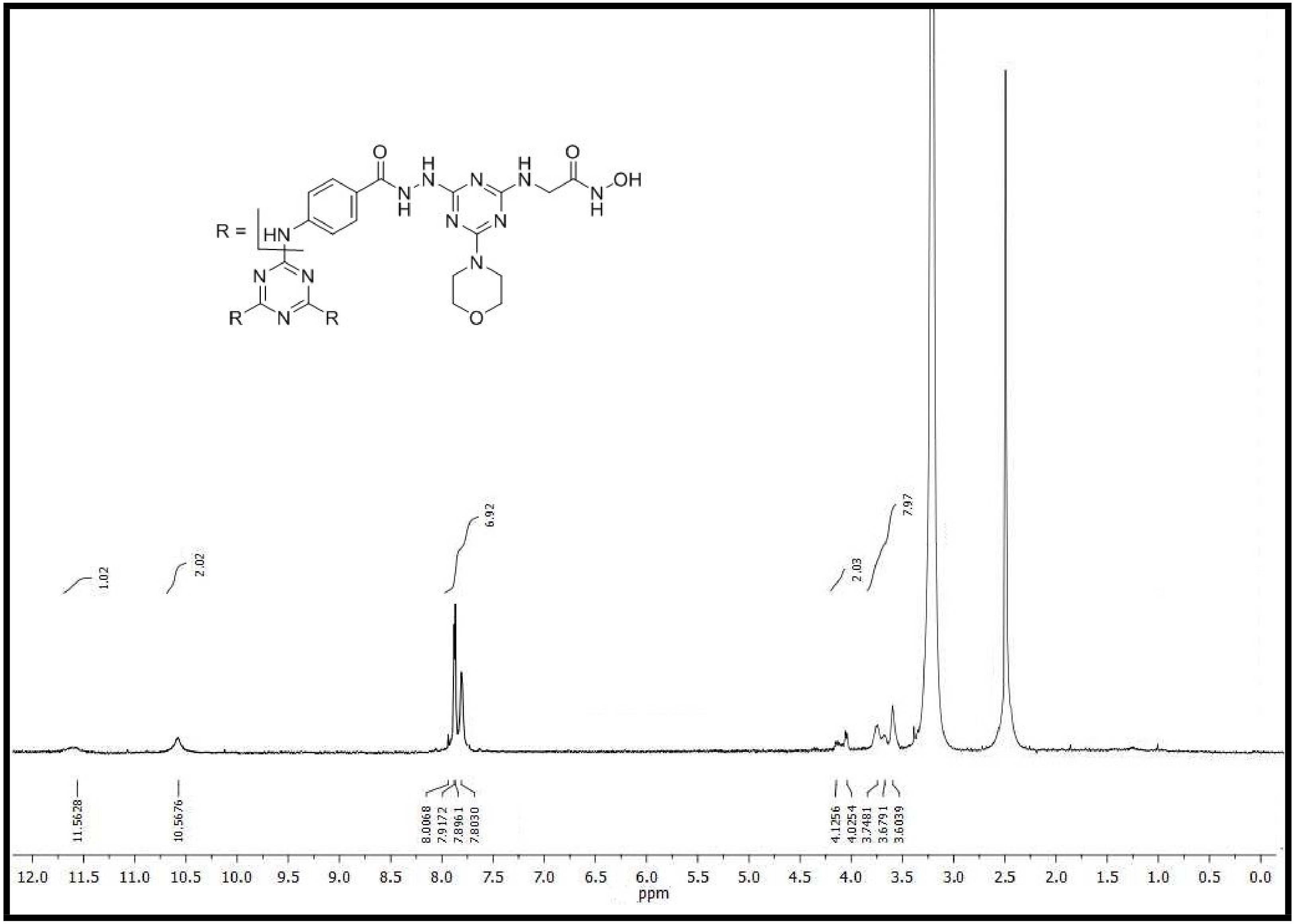

Figure S34 ^{1}H-NMR (DMSO-d_6) spectrum of 2,2',2''-((6,6',6''-(2,2',2''-(4,4',4''-((1,3,5-triazine-2,4,6-triyl)tris(azanediyl))tris(benzoyl))tris(hydrazine-2,1-diyl))tris (4-(morpholin-4-yl)-1,3,5-triazine-6,2-diyl))tris(azanediyl))tris(*N*-hydroxyacetamide) **14c**.

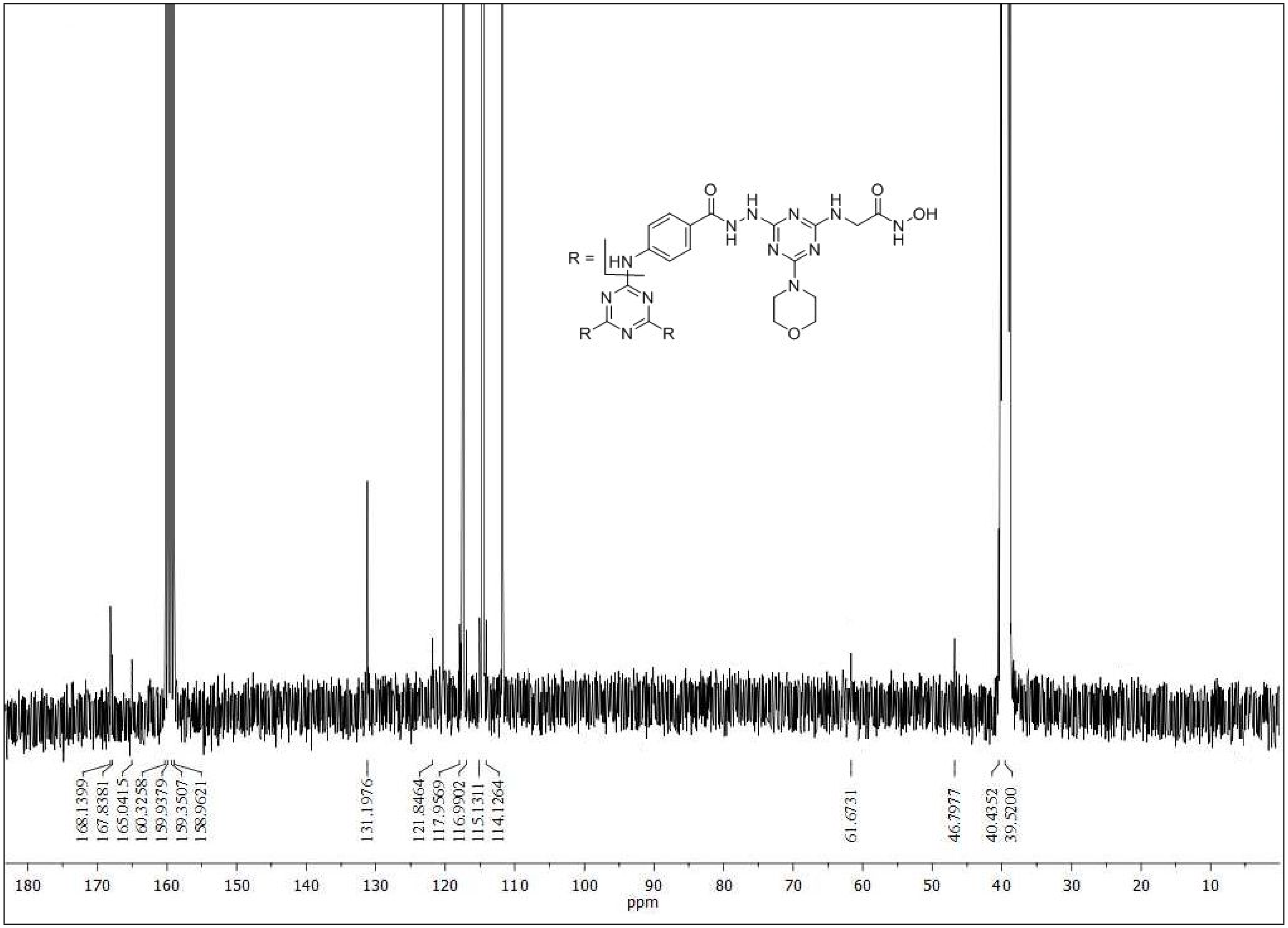

Figure S35: ^{13}C-NMR (DMSO-d_6, TFA) spectrum of 2,2',2''-((6,6',6''-(2,2',2''-(4,4',4''-((1,3,5-triazine-2,4,6-triyl)tris(azanediyl))tris(benzoyl))tris(hydrazine-2,1-diyl))tris(4-(morpholin-4-yl)-1,3,5-triazine-6,2-diyl))tris(azanediyl))tris(*N*-hydroxyacetamide) **14c**.

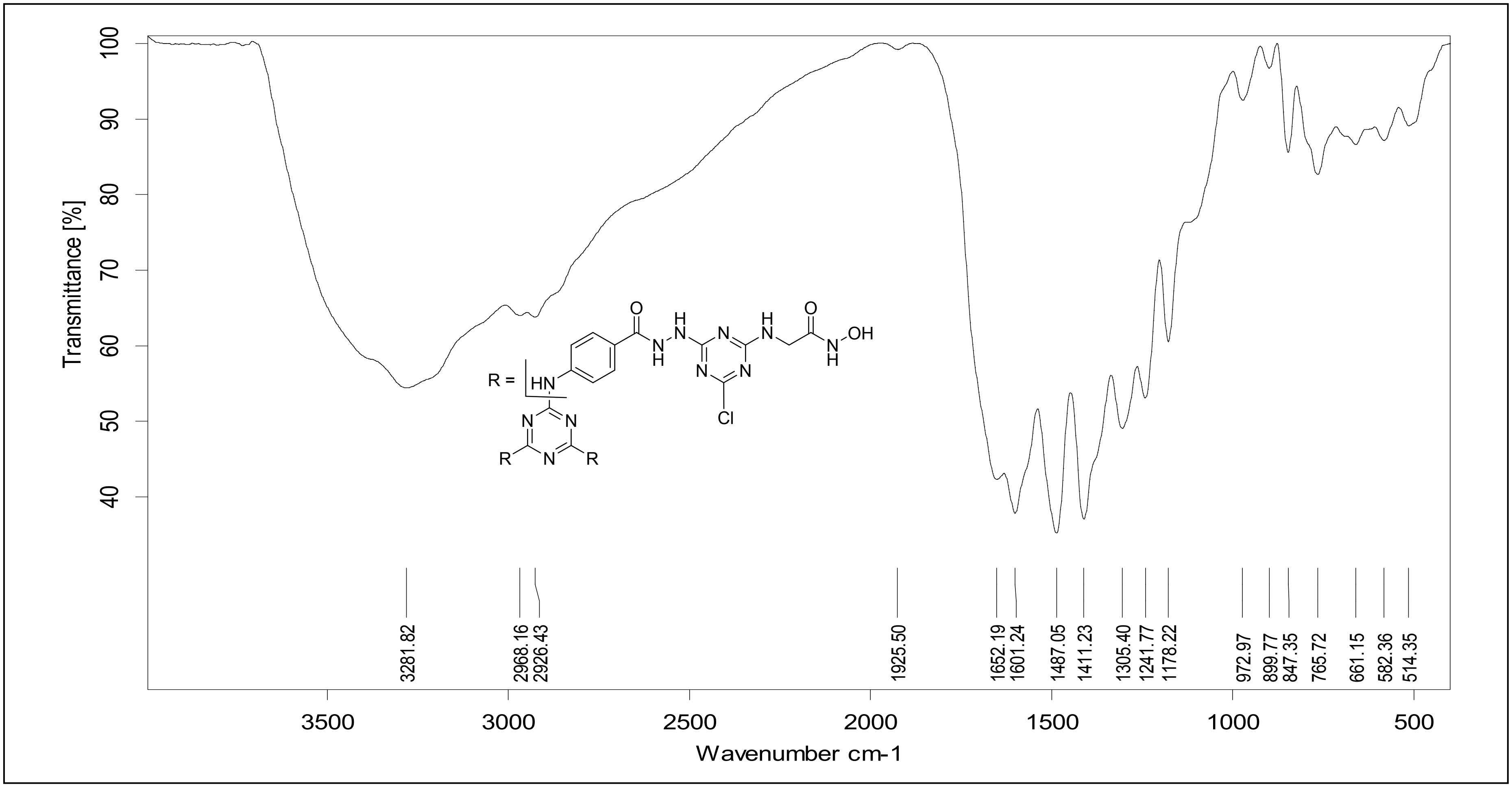

Figure S36: IR (KBr) spectrum of 2,2',2''-((6,6',6''-(2,2',2''-(4,4',4''-((1,3,5-triazine-2,4,6-triyl)tris(azanediyl))tris(benzoyl))tris(hydrazine-2,1-diyl))tris(4-chloro-1,3,5-triazine-6,2-diyl))tris(azanediyl))tris(*N*-hydroxyacetamide) **14d**.

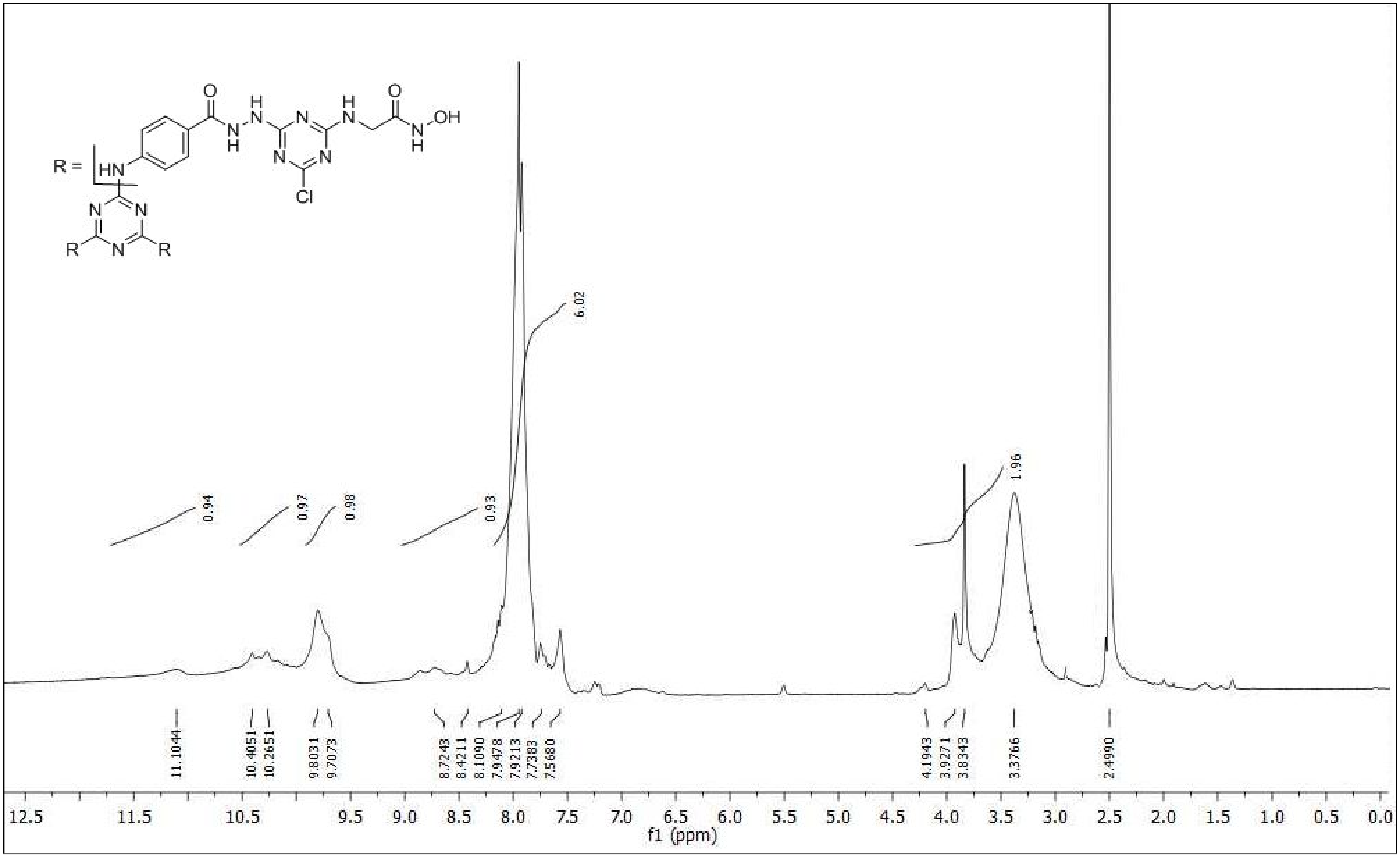

Figure S37: [1]H-NMR (DMSO-d_6) spectrum of 2,2',2''-((6,6',6''-(2,2',2''-(4,4',4''-((1,3,5-triazine-2,4,6-triyl)tris(azanediyl))tris(benzoyl))tris(hydrazine-2,1-diyl))tris(4-chloro-1,3,5-triazine-6,2-diyl))tris(azanediyl))tris(*N*-hydroxyacetamide) **14d**.

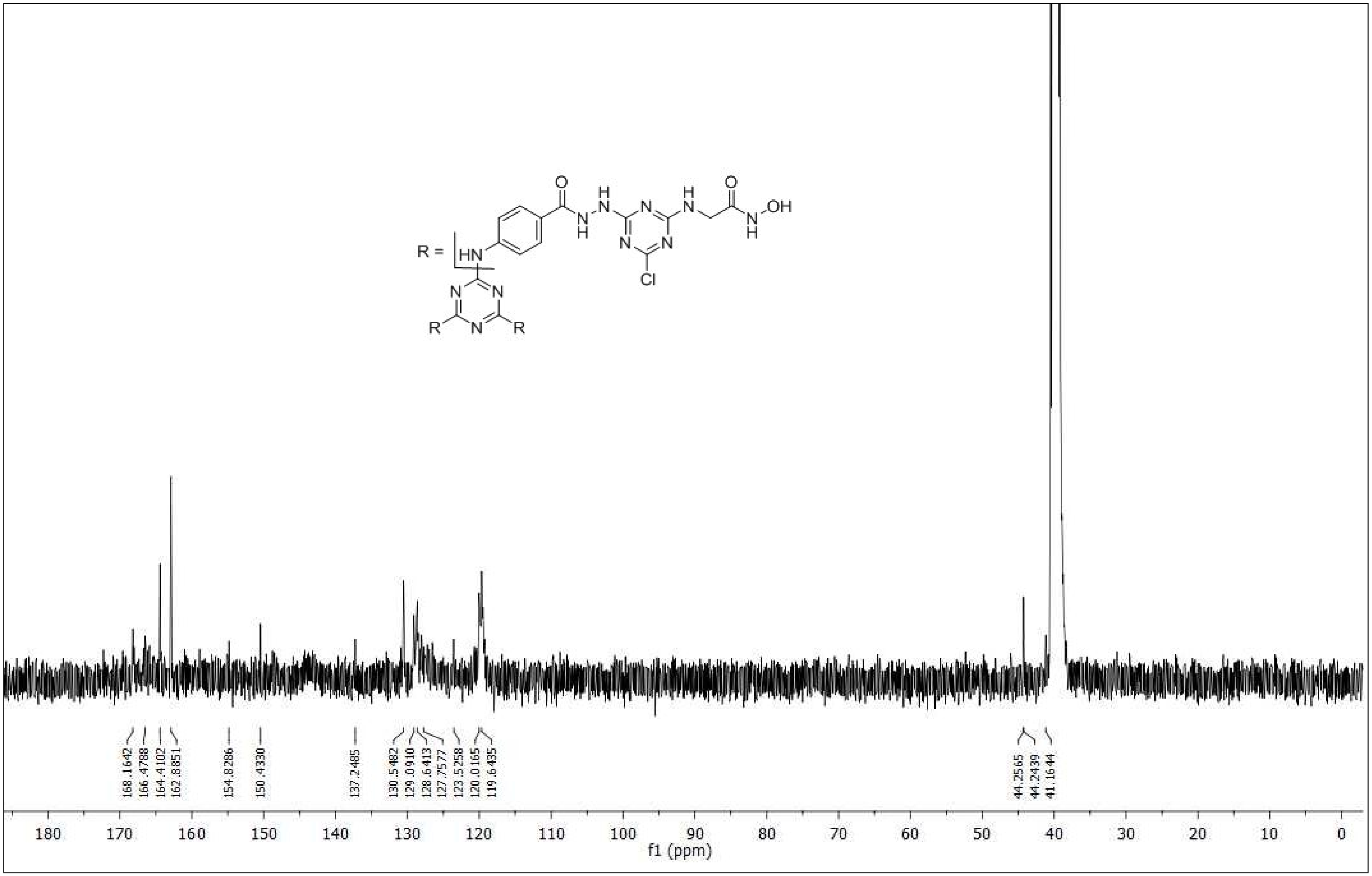

Figure S38: ^{13}C-NMR (DMSO-d_6) spectrum of 2,2',2''-((6,6',6''-(2,2',2''-(4,4',4''-((1,3,5-triazine-2,4,6-triyl)tris(azanediyl))tris(benzoyl))tris(hydrazine-2,1-diyl))tris(4-chloro-1,3,5-triazine-6,2-diyl))tris(azanediyl))tris(*N*-hydroxyacetamide) **14d**.

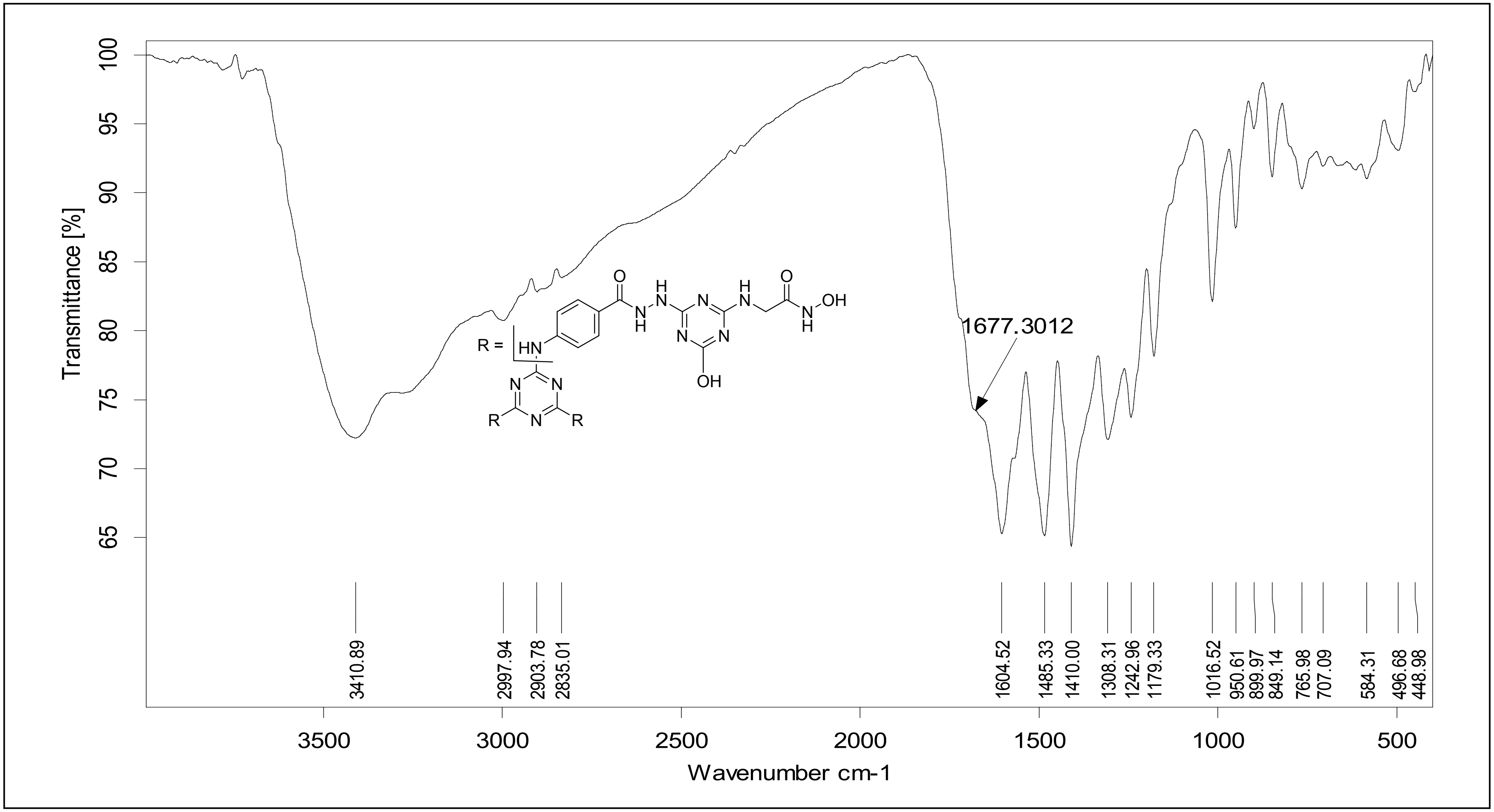

Figure S39: IR (KBr) spectrum of 2,2',2''-((6,6',6''-(2,2',2''-(4,4',4''-((1,3,5-triazine-2,4,6-triyl)tris(azanediyl))tris(benzoyl))tris(hydrazine-2,1-diyl))tris(4-hydroxy-1,3,5-triazine-6,2-diyl))tris(azanediyl))tris(*N*-hydroxyacetamide) **14e**.

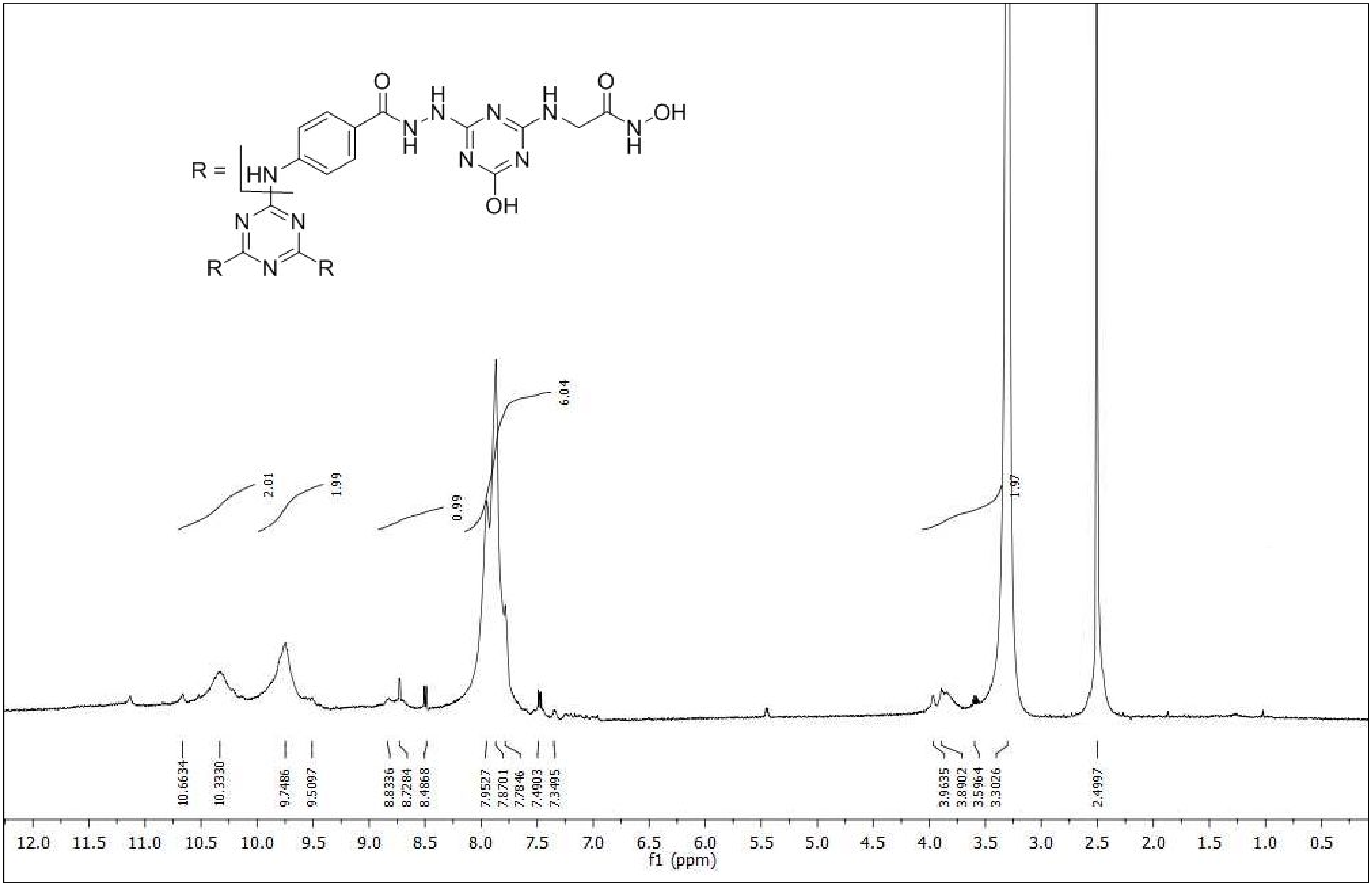

Figure S40: [1]H-NMR (DMSO-d_6) spectrum of 2,2',2''-((6,6',6''-(2,2',2''-(4,4',4''-((1,3,5-triazine-2,4,6-triyl)tris(azanediyl))tris(benzoyl))tris(hydrazine-2,1-diyl))tris(4-hydroxy-1,3,5-triazine-6,2-diyl))tris(azanediyl))tris(*N*-hydroxyacetamide) **14e**.

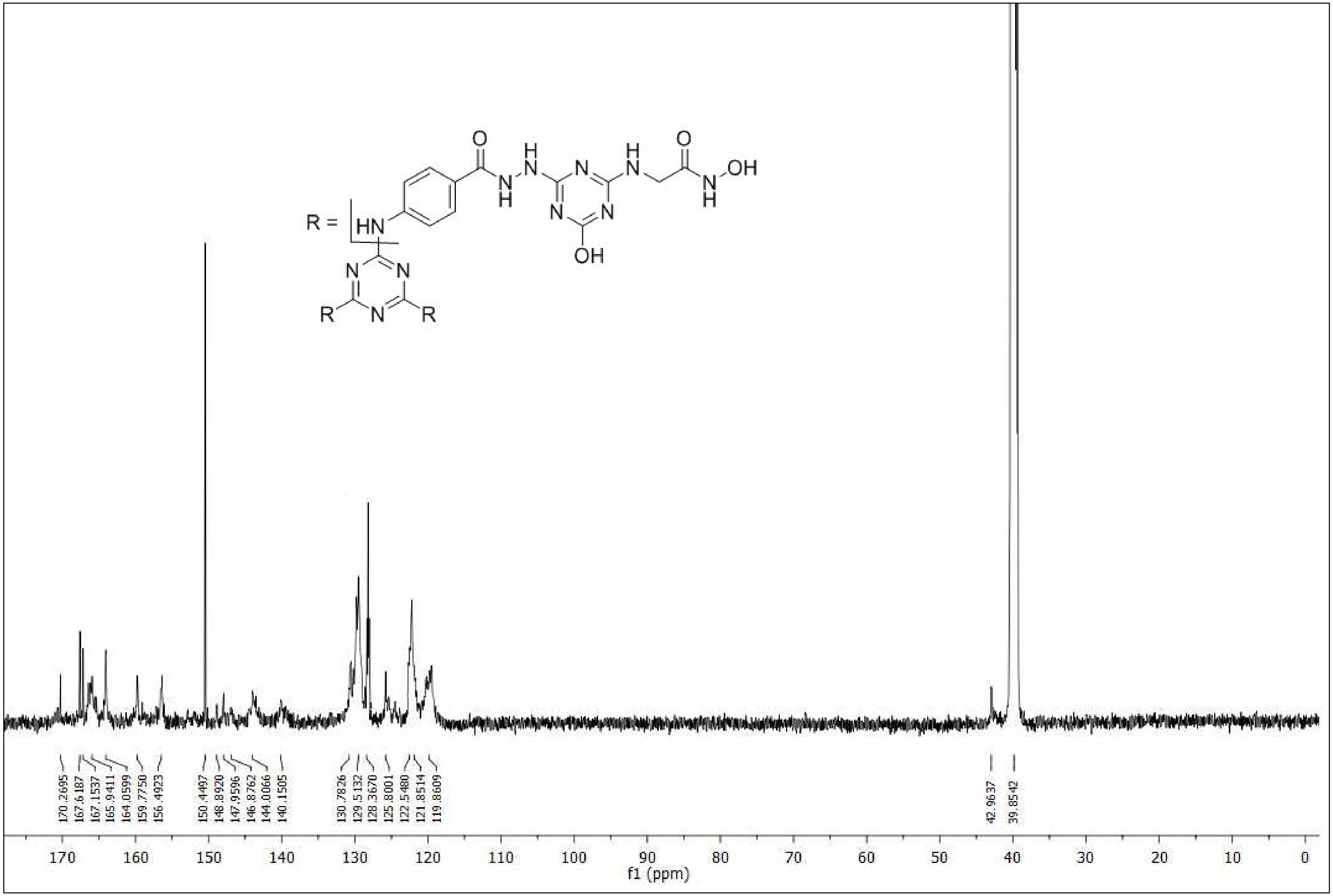

Figure S41: ^{13}C-NMR (DMSO-d_6) spectrum of 2,2',2''-((6,6',6''-(2,2',2''-(4,4',4''-((1,3,5-triazine-2,4,6-triyl)tris(azanediyl))tris(benzoyl))tris(hydrazine-2,1-diyl))tris(4-hydroxy-1,3,5-triazine-6,2-diyl))tris(azanediyl))tris(*N*-hydroxyacetamide) **14e**.

2. Biological evaluation

2.1. Cytotoxicity of the synthesized dendrimers on normal human lung fibroblasts (Wi-38)

Wi-38 cell line was cultured in DMEM medium-contained 10% fetal bovine serum (FBS), seeded as $5x10^3$ cells per well in 96-well cell culture plate and incubated at 37ºC in 5% CO_2 incubator. After 24 h for cell attachment, serial concentrations of the tested compounds were incubated with Wi-38 cells for 72 h. Cell viability was assayed by MTT method [1]. Twenty microliters of 5 mg/ml MTT (Sigma, USA) was added to each well and the plate was incubated at 37ºC for 3 h. Then MTT solution was removed, 100 µl DMSO was added and the absorbance of each well was measured with a microplate reader (BMG LabTech, Germany) at 570 nm. The effective safe concentration (EC_{100}) value (at 100% cell viability) of the tested compounds was estimated by the Graphpad Instat software.

2.2 Anticancer evaluation of the synthesized dendrimers

Anticancer activities of the synthesized dendrimers were evaluated on two human cancer cell lines namely; triple negative breast cancer cells; MDA-MB 231 and colon cancer cells; Caco-2, in comparison to reference chemotherapy. Triple negative breast cancer cells MDA-MB 231were cultured in RPMI-1640 (Lonza, USA) supplemented with 10% FBS, while colon cancer cell line (Caco-2) was cultured in DMEM (Lonza, USA) contained with 10% FBS. All cancer cells ($4x10^3$ cells/well) were seeded in sterile 96-well plates. After 24h, serial concentrations of the tested compounds were incubated with the cancer cell lines for 72 h at 37ºC in 5% CO_2 incubator. MTT method was done as described above. The half maximal inhibitory concentration (IC_{50}) values were calculated using the Graphpad Instat software. Furthermore, cellular morphological changes before and after treatment with the most effective and safest anticancer compounds were investigated using phase contrast inverted microscope with a digital camera (Olympus, Japan).

2.3. In vitro MMPs inhibition of the most active dendrimers

- The assay protocols were performed as directed ny the manufacturer
- Inhibition data analyses was carried out as follows:

MMP-9 inhibition

code	IC50	conc.uM	log conc	%inh	T2	T1	ΔT	RFU2	RFU1	ΔRFU	slope	K.Activity	EC
8a		10	4	89.7	30	0	30	0.145	0	0.145	0.0469	12.367	120
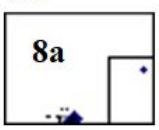		1	3	76.4	30	0	30	0.332	0	0.332	0.0469	28.316	120
		0.1	2	42.7	30	0	30	0.806	0	0.806	0.0469	68.742	120
		0.01	1	20.7	30	0	30	1.116	0	1.116	0.0469	95.181	120
EC				0	30	0	30	1.407	0	1.407	0.0469	120	120

code	IC50	conc.uM	log conc	%inh	T2	T1	ΔT	RFU2	RFU1	ΔRFU	slope	K.Activity	EC
14a		10	4	81.4	30	0	30	0.261	0	0.261	0.0469	22.26	120
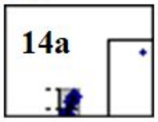		1	3	64.9	30	0	30	0.494	0	0.494	0.0469	42.132	120
		0.1	2	31.8	30	0	30	0.959	0	0.959	0.0469	81.791	120
		0.01	1	15.1	30	0	30	1.194	0	1.194	0.0469	101.83	120
EC				0	30	0	30	1.407	0	1.407	0.0469	120	120

code	IC50	conc.uM	log conc	%inh	T2	T1	ΔT	RFU2	RFU1	ΔRFU	slope	K.Activity	EC
14b		10	4	88.3	30	0	30	0.165	0	0.165	0.0469	14.072	120
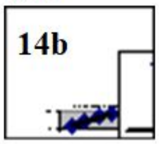		1	3	71.2	30	0	30	0.405	0	0.405	0.0469	34.542	120
		0.1	2	42.4	30	0	30	0.811	0	0.811	0.0469	69.168	120
		0.01	1	16.1	30	0	30	1.181	0	1.181	0.0469	100.72	120
EC				0	30	0	30	1.407	0	1.407	0.0469	120	120

code	IC50	conc.ug/ml	log conc	%inh	T2	T1	ΔT	RFU2	RFU1	ΔRFU	slope	K.Activity	EC
14 d		10	4	87.7	30	0	30	0.173	0	0.173	0.0469	14.755	120
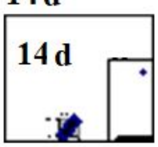		1	3	70.3	30	0	30	0.418	0	0.418	0.0469	35.65	120
		0.1	2	34.1	30	0	30	0.927	0	0.927	0.0469	79.062	120
		0.01	1	18.9	30	0	30	1.141	0	1.141	0.0469	97.313	120
EC				0	30	0	30	1.407	0	1.407	0.0469	120	120

code	IC50	conc.uM	log conc	%inh	T2	T1	ΔT	RFU2	RFU1	ΔRFU	slope	K.Activity	EC
NNGH		10	4	75.37526	30	0	30	0.115	0	0.115	0.015567	29.54969	120
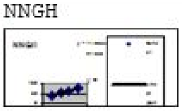		1	3	63.81234	30	0	30	0.169	0	0.169	0.015567	43.42519	120
		0.1	2	50.53639	30	0	30	0.231	0	0.231	0.015567	59.35633	120
		0.01	1	40.25824	30	0	30	0.279	0	0.279	0.015567	71.69011	120
EC				0	30	0	30	0.467	0	0.467	0.015567	120	120

MMP-2 inhibition

code	IC_{50}	conc.ng/ml	log conc	%inh	T2	T1	ΔT	RFU2	RFU1	ΔRFU	slope	K.Activity	EC
8a		10	1	76	30	0	30	24.31	0	24.31	3.33333	29.17	120
		1	0	56	30	0	30	43.86	0	43.86	3.33333	52.63	120
		0.1	-1	30	30	0	30	69.75	0	69.75	3.33333	83.7	120
		0.01	-2	12	30	0	30	88.12	0	88.12	3.33333	105.7	120
EC				0	30	0	30	100	0	100	3.33333	120	120

code	IC_{50}	conc.ng/ml	log conc	%inh	T2	T1	ΔT	RFU2	RFU1	ΔRFU	slope	K.Activity	EC
14a		10	1	74	30	0	30	25.99	0	25.99	3.33333	31.19	120
		1	0	57	30	0	30	42.64	0	42.64	3.33333	51.17	120
		0.1	-1	27	30	0	30	72.57	0	72.57	3.33333	87.08	120
		0.01	-2	8.3	30	0	30	91.74	0	91.74	3.33333	110.1	120
EC				0	30	0	30	100	0	100	3.33333	120	120

code	IC50	conc.ng/ml	log conc	%inh	T2	T1	ΔT	RFU2	RFU1	ΔRFU	slope	K.Activity	EC
14b		10	1	86	30	0	30	13.62	0	13.62	3.33333	16.34	120
		1	0	70	30	0	30	29.81	0	29.81	3.33333	35.77	120
		0.1	-1	48	30	0	30	52.41	0	52.41	3.33333	62.89	120
		0.01	-2	33	30	0	30	66.93	0	66.93	3.33333	80.32	120
EC				0	30	0	30	100	0	100	3.33333	120	120

code	IC50	conc.ng/ml	log conc	%inh	T2	T1	ΔT	RFU2	RFU1	ΔRFU	slope	K.Activity	EC
14d		10	1	82	30	0	30	17.52	0	17.52	3.33333	21.02	120
		1	0	54	30	0	30	46.32	0	46.32	3.33333	55.58	120
		0.1	-1	28	30	0	30	72.42	0	72.42	3.33333	86.9	120
		0.01	-2	15	30	0	30	85.07	0	85.07	3.33333	102.1	120
EC				0	30	0	30	100	0	100	3.33333	120	120

code	IC50	conc.ng/ml	log conc	%inh	T2	T1	ΔT	RFU2	RFU1	ΔRFU	slope	K.Activity	EC
NNGH		10	1	89	30	0	30	11.41	0	11.41	3.33333	13.69	120
		1	0	72	30	0	30	28.45	0	28.45	3.33333	34.14	120
		0.1	-1	49	30	0	30	51.16	0	51.16	3.33333	61.39	120
		0.01	-2	35	30	0	30	64.58	0	64.58	3.33333	77.5	120
EC				0	30	0	30	100	0	100	3.33333	120	120

MMP-7 inhibition

code	IC_{50}	conc	log	%inh	T2	T1	ΔT	RFU2	RFU1	ΔRFU	slope	K.Activity
8a		10	1	81	30	0	30	19.14	0	19.14	3.333	22.96802
		1	0	66	30	0	30	33.89	0	33.89	3.333	40.66804
		0.1	-1	44	30	0	30	56.27	0	56.27	3.333	67.52407
		0.01	-2	25	30	0	30	75.43	0	75.43	3.333	90.51609
EC				0	30	0	30	100	0	100	3.333	120

code	IC50	conc.uM	log conc	%inh	T2	T1	ΔT	RFU2	RFU1	ΔRFU	slope	K.Activity	EC
NNGH													
		10	4	89.73602	30	0	30	17843	0	17843	5794.7	12.31677	120
		1	3	76.23921	30	0	30	41306	0	41306	5794.7	28.51295	120
		0.1	2	40.40991	30	0	30	103592	0	103592	5794.7	71.5081	120
		0.01	1	7.055873	30	0	30	161575	0	161575	5794.7	111.533	120
EC				0	30	0	30	173841	0	173841	5794.7	120	120

MMP-10 inhibition

code	IC_{50}	conc.ng/ml	log conc	%inh	T2	T1	ΔT	RFU2	RFU1	ΔRFU	slope	K.Activity
8a		10	1	85	30	0	30	14.61	0	14.61	3.333	17.53202
		1	0	64	30	0	30	35.55	0	35.55	3.333	42.66004
		0.1	-1	47	30	0	30	52.58	0	52.58	3.333	63.09606
		0.01	-2	28	30	0	30	71.79	0	71.79	3.333	86.14809
EC				0	30	0	30	100	0	100	3.333	120

code	IC50	conc.uM	log conc	%inh	T2	T1	ΔT	RFU2	RFU1	ΔRFU	slope	K.Activity	EC
NNGH		10	4	92.93016	30	0	30	11059	0	11059	5214.167	8.48381	120
		1	3	82.3596	30	0	30	27594	0	27594	5214.167	21.16848	120
		0.1	2	46.52901	30	0	30	83642	0	83642	5214.167	64.16519	120
		0.01	1	25.27346	30	0	30	116891	0	116891	5214.167	89.67185	120
EC				0	30	0	30	156425	0	156425	5214.167	120	120

MMP-13 inhibition

code	IC50	conc.ng/ml	log conc	%inh	T2	T1	ΔT	RFU2	RFU1	ΔRFU	slope	K.Activity
8a		10	1	89	30	0	30	11.21	0	11.21	3.333	13.45201
		1	0	74	30	0	30	25.91	0	25.91	3.333	31.09203
		0.1	-1	46	30	0	30	53.83	0	53.83	3.333	64.59606
		0.01	-2	26	30	0	30	74.01	0	74.01	3.333	88.81209
EC				0	30	0	30	100	0	100	3.333	120

code	IC50	conc.uM	log conc	%inh	T2	T1	ΔT	RFU2	RFU1	ΔRFU	slope	K.Activity	EC
NNGH		10	4	87.3909	30	0	30	17597	0	17597	4651.933	15.13091	120
		1	3	65.43444	30	0	30	48239	0	48239	4651.933	41.47867	120
		0.1	2	31.01864	30	0	30	96269	0	96269	4651.933	82.77763	120
		0.01	1	10.09114	30	0	30	125475	0	125475	4651.933	107.8906	120
EC				0	30	0	30	139558	0	139558	4651.933	120	120

2.4. Flow cytometric analysis of apoptotic effects of the most active and safe compounds

Dendrimers were incubated, for 72 h, with MDA-MB231 and Caco-2. After trypsinization, the untreated and treated cells were incubated with annexin V/PI for 15 min. Then cells were fixed and incubated with streptavidin-fluorescein (5 µg/mL) for 15 min. The apoptosis-dependent anticancer effect was determined by quantification of annexin-stained apoptotic cells using the FITC signal detector (FL1) against the phycoerythrin emission signal detector (FL2).

2.5. Tumor cell migration inhibition

Caco2 cells were used for the wound healing migration assay. After cell seeding in 6-well plate and reaching > 90% confluence, a yellow tip was used for scratching. Then cells were washed and treated with the selected compounds. The wound area was photographed and calculated by image j software for estimating the inhibition migration percentages in the treated wells relative to untreated wells.

2.6. Expression of VEGF, cyclin D and p21

Total RNAs of untreated and three most effective anticancer compounds-treated MDA-MB-231 and Caco-2 cells were extracted using Gene JET RNA Purification Kit (Thermo Scientific, USA). The cDNA was synthesized from mRNA using cDNA Synthesis Kit (Thermo Scientific, USA). Real time PCR was performed using SYBR green master mix and specific primers (Forward/Reverse) were 5′-TACTCTGGCGCAGAAATTAGGTC-3′/5′-CTGTCTCGGAGCTCGTCTATTTG-3′, 5′-CCACAGCGATATCCAGACATTC-3′/5′-GAAGTCAAAGTTCCACCGTTCTC-3′ and 5′-GAGGGCAGAATCATCACGAAG-3′/5′-CACACAGGATGGCTTGAAGA-3′ for cyclin D, p21 and VEGF genes, respectively. The $2^{-\Delta\Delta CT}$ equation was used to estimate the change in gene expressions in the treated cancer cells relative to untreated cancer cells.

2.7. Statistical analysis

The data are expressed as mean ± standard error of mean (SEM) and the significant values were considered at *p*< 0.05. One-way analysis of variance (ANOVA) by Tukey’s test used for evaluating the difference between the mean values of the studied treatments. The analysis was done for three measurements using SPSS software version 16.

References:

[1] T. Mosmann, J. Immunol. Methods 65 (1–2) (1983) 55–63.